[18] Serrano, M., Hannon, G.J. and Beach, D.A. (1993) "A new regulatory motif in cell-cycle control causing specific inhibition of cyclin D/CDK4", *Nature* **366**, 704–707.
[19] Capon, D.J., Chen, E.Y., Levinson, A.D., Seeburg, P.H. and Goeddel, D.V. (1983) "Complete nucleotide sequences of the T24 human bladder carcinoma oncogene and its normal homologue", *Nature* **302**, 33–37.
[20] Yamashita, N., Murata, M., Inoue, S., Hiraku, Y., Yoshinaga, T. and Kawanishi, S. (1998) "Superoxide formation and DNA damage induced by a fragrant furanone in the presence of copper(II)", *Mutat. Res.* **397**, 191–201.
[21] Oikawa, S., Murakami, K. and Kawanishi, S. (2003) "Oxidative damage to cellular and isolated DNA by homocysteine: implications for carcinogenesis", *Oncogene* **22**, 3530–3538.
[22] Yamamoto, K. and Kawanishi, S. (1989) "Hydroxyl free radical is not the main active species in site specific DNA damage induced by copper(II) ion and hydrogen peroxide", *J. Biol. Chem.* **264**, 15435–15440.
[23] Maxam, A.M. and Gilbert, W. (1980) "Sequencing end-labeled DNA with base-specific chemical cleavages", *Meth. Enzymol.* **65**, 499–560.
[24] Kasai, H., Grain, P.F., Kuchino, Y., Nishimura, S., Ootsuyama, A. and Tanooka, H. (1986) "Formation of 8-hydroxyguanine moiety in cellular DNA by agents producing oxygen radicals and evidence for its repair", *Carcinogenesis* **7**, 1849–1851.
[25] Ito, K., Inoue, S., Yamamoto, K. and Kawanishi, S. (1993) "8-Hydroxydeoxyguanosine formation at the 5′ site of 5′-GG-3′ sequence in double-stranded DNA by UV radiation with riboflavin", *J. Biol. Chem.* **268**, 13221–13227.
[26] Blair, D. and Diel, H. (1961) "Bathophenanthrolinedisulphonic acid and bathocuproinedisulphonic acid, water soluble reagents for iron and copper", *Talanta* **7**, 163–174.
[27] David-Cordonnier, M.H., Laval, J. and O'Neill, P. (2000) "Clustered DNA damage, influence on damage excision by XRS5 nuclear extracts and *Escherichia coli* Nth and Fpg proteins", *J. Biol. Chem.* **275**, 11865–11873.
[28] D'Ham, C., Romieu, A., Jaquinod, M., Gasparutto, D. and Cadet, J. (1999) "Excision of 5,6-dihydroxy-5,6-dihydrothymine, 5,6-dihydrothymine, and 5-hydroxycytosine from defined sequence oligonucleotides by *Escherichia coli* endonuclease III and Fpg proteins: kinetic and mechanistic aspects", *Biochemistry* **38**, 3335–3344.
[29] Bourdat, A.-G., Douki, T., Frelon, S., Gasparutto, D. and Cadet, J. (2000) "Tandem base lesions are generated by hydroxyl radical within isolated DNA in aerated aqueous solution", *J. Am. Chem. Soc.* **122**, 4549–4556.
[30] Box, H.C., Budzinski, E.E., Dawidzik, J.B., Gobey, J.S. and Freund, H.G. (1997) "Free radical-induced tandem base damage in DNA oligomers", *Free Radic. Biol. Med.* **23**, 1021–1030.
[31] Frelon, S., Douki, T., Favier, A. and Cadet, J. (2003) "Hydroxyl radical is not the main reactive species involved in the degradation of DNA bases by copper in the presence of hydrogen peroxide", *Chem. Res. Toxicol.* **16**, 191–197.
[32] Lee, D.H., O'Connor, T.R. and Pfeifer, G.P. (2002) "Oxidative DNA damage induced by copper and hydrogen peroxide promotes CG ⇒ TT tandem mutations at methylated CpG dinucleotides in nucleotide excision repair-deficient cells", *Nucleic Acids Res.* **30**, 3566–3573.
[33] Blaisdell, J.O. and Wallace, S.S. (2001) "Abortive base-excision repair of radiation-induced clustered DNA lesions in *Escherichia coli*", *Proc. Natl Acad. Sci. USA* **98**, 7426–7430.
[34] Youngman, R.J. and Elstner, E.F. (1981) "Oxygen species in paraquat toxicity: the crypto-OH radical", *FEBS Lett.* **129**, 265–268.
[35] Kawanishi, S., Hiraku, Y. and Oikawa, S. (2001) "Mechanism of guanine-specific DNA damage by oxidative stress and its role in carcinogenesis and aging", *Mutat. Res.* **488**, 65–76.
[36] Hirakawa, K., Oikawa, S., Hirkaku, Y., Hirosawa, I. and Kawanishi, S. (2002) "Catechol and hydroquinone have different redox properties responsible for their differential DNA-damaging ability", *Chem. Res. Toxicol.* **15**, 76–82.
[37] Dijkwel, P.A. and Wenink, P.W. (1986) "Structural integrity of the nuclear matrix: differential effects of thiol agents and metal chelators", *J. Cell Sci.* **84**, 53–67.
[38] Saucier, M.A., Wang, X., Re, R.N., Brown, J. and Bryan, S.E. (1991) "Effects of ionic strength on endogenous nuclease activity in chelated and nonchelated chromatin", *J. Inorg. Biochem.* **41**, 117–124.
[39] Theophanides, T. and Anastassopoulou, J. (2002) "Copper and carcinogenesis", *Crit. Rev. Oncol. Hematol.* **42**, 57–64.
[40] Bar-Or, D., Thomas, G.W., Rael, L.T., Lau, E.P. and Winkler, J.V. (2001) "Asp-Ala-His-Lys (DAHK) inhibits copper-induced oxidative DNA double strand breaks and telomere shortening", *Biochem. Biophys. Res. Commun.* **282**, 356–360.
[41] Linder, M.C. (2001) "Copper and genomic stability in mammals", *Mutat. Res.* **475**, 141–152.
[42] Ishibashi, K., Fujishima, A., Watanabe, T. and Hashimoto, K. (2000) "Quantum yields of active oxidative species formed on TiO_2 photocatalyst", *J. Photochem. Photobiol. A Chem.* **134**, 139–142.
[43] Akhlynina, T.V., Jans, D.A., Rosenkranz, A.A., Statsyuk, N.V., Balashova, I.Y., Toth, G., Pavo, I., Rubin, A.B. and Sobolev, A.S. (1997) "Nuclear targeting of chlorin e6 enhances its photosensitizing activity", *J. Biol. Chem.* **272**, 20328–20331.
[44] Bisland, S.K., Singh, D. and Gariepy, J. (1999) "Potentiation of chlorin e6 photodynamic activity *in vitro* with peptide-based intracellular vehicles", *Bioconjug. Chem.* **10**, 982–992.

Available online at www.sciencedirect.com
SCIENCE DIRECT®
Mutation Research 558 (2004) 111–120
Genetic Toxicology and Environmental Mutagenesis
www.elsevier.com/locate/gentox
Community address: www.elsevier.com/locate/mutres

Metal-mediated oxidative damage to cellular and isolated DNA by gallic acid, a metabolite of antioxidant propyl gallate

Hatasu Kobayashi[a], Shinji Oikawa[a], Kazutaka Hirakawa[b], Shosuke Kawanishi[a,*]

[a] *Department of Environmental and Molecular Medicine, Mie University School of Medicine, Edobashi 2-174, Tsu, Mie 514-8507, Japan*
[b] *Department of Radiation Chemistry, Life Science Research Center, Mie University, Edobashi 2-174, Tsu, Mie 514-8507, Japan*

Received 26 August 2003; received in revised form 18 November 2003; accepted 18 November 2003

Abstract

Propyl gallate (PG), widely used as an antioxidant in foods, is carcinogenic to mice and rats. PG increased the amount of 8-oxo-7,8-dihydro-2′-deoxyguanosine (8-oxodG), a characteristic oxidative DNA lesion, in human leukemia cell line HL-60, but not in HP100, which is hydrogen peroxide (H_2O_2)-resistant cell line derived from HL-60. Although PG induced no or little damage to ^{32}P-5′-end-labeled DNA fragments obtained from genes that are relevant to human cancer, DNA damage was observed with treatment of esterase. HPLC analysis of the products generated from PG incubated with esterase revealed that PG converted into gallic acid (GA). GA induced DNA damage in a dose-dependent manner in the presence of Fe(III)EDTA or Cu(II). In the presence of Fe(III) complex such as Fe(III)EDTA or Fe(III)ADP, GA caused DNA damage at every nucleotide. Fe(III) complex-mediated DNA damage by GA was inhibited by free hydroxy radical (•OH) scavengers, catalase and an iron chelating agent. These results suggested that the Fe(III) complex-mediated DNA damage caused by GA is mainly due to •OH generated via the Fenton reaction. In the presence of Cu(II), DNA damage induced by GA occurred at thymine and cytosine. Although •OH scavengers did not prevent the DNA damage, methional inhibited the DNA damage. Cu(II)-mediated DNA damage was inhibited by catalase and a Cu(I) chelator. These results indicated that reactive oxygen species formed by the interaction of Cu(I) and H_2O_2 participates in the DNA damage. GA increased 8-oxodG content in calf thymus DNA in the presence of Cu(II), Fe(III)EDTA or Fe(III)ADP. This study suggested that metal-mediated DNA damage caused by GA plays an important role in the carcinogenicity of PG.

Keywords: DNA damage; Propyl gallate; Gallic acid; 8-Oxo-7,8-dihydro-2′-deoxyguanosine; Reactive oxygen species; Copper; Iron

1. Introduction

Propyl gallate (PG) is widely used as an antioxidant in the food industry. PG has been investigated as a potential chemopreventive agent in several animal experiments [1–3]. Thus, PG is recognized as being the important synthetic antioxidant. In contrast, National Toxicology Program (NTP) reported that PG induced preputial gland tumors, islet-cell tumors of the pancreas, and pheochromocytomas of the adrenal glands in male rats [4]. PG also induced malignant lymphoma

Abbreviations: PG, propyl gallate; 8-oxodG, 8-oxo-7,8-dihydro-2′-deoxyguanosine (also known as 8-hydroxy-2′-deoxyguanosine); GA, gallic acid; CIP, calf intestine phosphatase; DTPA, diethylenetriamine-*N*,*N*,*N*′,*N*″,*N*″-pentaacetic acid; DMSO, dimethylsulfoxide; BAP, bacterial alkaline phosphatase; SOD, superoxide dismutase; HPLC-ECD, an electrochemical detector coupled to high-performance liquid chromatography; HOMO, highest occupied molecular orbital

* Corresponding author. Tel.: +81-59-231-5011; fax: +81-59-231-5011.
E-mail address: kawanisi@doc.medic.mie-u.ac.jp (S. Kawanishi).

1383-5718/$ – see front matter © 2003 Elsevier B.V. All rights reserved.
doi:10.1016/j.mrgentox.2003.11.002

in male mice [4]. In rat, co-administration of $NaNO_2$ with PG promoted forestomach carcinogenesis after initiation with *N*-methyl-*N'*-nitro-*N*-nitrosoguanidine [5]. It is reported that PG is not easily excreted and tends to accumulate in the body [6]. As measured by the Salmonella/microsome mutagenesis assay, PG caused an enhancement of the mutagenic activities of the carcinogens *N*-hydroxy-2-acetylaminofluorene and 4-nitroquinoline 1-oxide [7]. PG induced sister-chromatid exchanges and chromosomal aberrations in CHO-K1 cells [8]. These reports have suggested that accumulation of PG may contribute to carcinogenesis. However, the mechanism leading to carcinogenesis has not yet been clarified.

To investigate the ability of PG to cause oxidative DNA damage, the amount of 8-oxo-7,8-dihydro-2'-deoxyguanosine (8-oxodG), a characteristic oxidative DNA lesion, induced by PG was measured in a human leukemia cell line, HL-60, and its hydrogen peroxide (H_2O_2)-resistant clone HP100 by using an electrochemical detector coupled to high-performance liquid chromatography (HPLC-ECD). 8-OxodG is known to cause DNA misreplication resulting in mutation or cancer [9,10]. It has been reported that PG in the hepatocyte suspensions is converted to gallic acid (GA) [6]. To make sure that PG is converted to GA, we analyzed products generated from PG incubated with esterase by using an HPLC equipped with a photodiode array. Furthermore, to clarify the mechanism of carcinogenesis by PG, we examined the DNA damage caused by PG, esterase-treated PG and GA in the presence of metal ions, using ^{32}P-5'-end-labeled DNA fragments obtained from the human *p16* and *p53* tumor suppressor genes. In addition, we analyzed the formation of 8-oxodG in calf thymus DNA caused by GA in the presence of metal ions.

2. Materials and methods

2.1. Materials

Restriction enzymes and calf intestine phosphatase (CIP) were purchased from Boehringer Mannheim GmbH (Germany). T4 polynucleotide kinase was from New England Biolabs (Beverly, MA). [γ-^{32}P]ATP was from New England Nuclear (Boston, MA). Diethylenetriamine-*N,N,N',N'',N''*-pentaacetic acid (DTPA) and bathocuproinedisulfonic acid were from Dojin Chemical Co. (Kumamoto, Japan). Acrylamide, dimethylsulfoxide (DMSO), bisacrylamide, piperidine, PG, and GA were from Wako Pure Chemical Industries (Osaka, Japan). $CuCl_2$, ethanol, D-mannitol, sodium formate, and proteinase K were from Nacalai Tesque (Kyoto, Japan). Calf thymus DNA, bacterial alkaline phosphatase (BAP, from *Escherichia coli*), superoxide dismutase (SOD, 3000 U/mg from bovine erythrocytes), catalase (45,000 U/mg from bovine liver), esterase (250 U/mg from porcine liver), and RNase A were from Sigma Chemical Co. (St. Louis, MO). Nuclease P1 was from Yamasa Shoyu Co. (Chiba, Japan). Lysis buffer for DNA extraction was from Applied Biosystems (Foster City, CA).

2.2. Measurement of 8-oxodG in cultured cell

Human leukemia HL-60 cells and its H_2O_2-resistant clone HP100 were grown in RPMI 1640 supplemented with 6% fetal bovine serum at 37 °C under 5% CO_2 in a humidified atmosphere. Cells (10^6 cells/ml) were incubated with PG for 2 h at 37 °C and immediately washed three times with phosphate-buffered saline. DNA was extracted under anaerobic condition digested to component nucleosides with nuclease P_1 and BAP and analyzed by HPLC-ECD [11,12].

2.3. Analysis of PG and its metabolite by HPLC

The reaction mixture containing 100 μM PG and 0.625 U esterase in 50 μl of 10 mM sodium phosphate buffer (pH 7.8) containing 5 μM DTPA was incubated at 37 °C. To analyze the products generated from PG incubated with esterase, HPLC was carried out on an LC-10A HPLC system (Shimadzu, Kyoto, Japan) using a Cosmosil column (Nacalai Tesque, 4.6 mm internal diameter × 150 mm), flow rate of 1 ml/min, linear gradient in 12.5 min of 0–50% acetonitrile. The HPLC eluate was routed directly into a photodiode array UV-Vis detector (SPD-M10A, Shimadzu) and the spectrum of the eluate was measured [13].

2.4. Preparation of ^{32}P-5'-end-labeled DNA fragments

Two fragments containing exon 1 or 2 of the human *p16* tumor suppressor gene [14] were obtained as described previously [15]. The 5'-end-labeled 490 bp

fragment (*Eco*RI* 5841–*Eco*RI* 6330) containing exon 1 was further digested with *Mro*I to obtain the singly labeled 328 bp fragment (*Eco*RI* 5841–*Mro*I 6168) and the 158 bp fragment (*Mro*I 6173–*Eco*RI* 6330). The 5′-end-labeled 460 bp fragment (*Eco*RI* 9481–*Eco*RI* 9940) containing exon 2 was also further digested with *Bss*H II to obtain the singly labeled 309 bp fragment (*Eco*RI* 9481–*Bss*H II 9789), and the 147 bp fragment (*Bss*H II 9794–*Eco*RI* 9940).

DNA fragments were also obtained from the human *p53* tumor suppressor gene [16]. The ^{32}P-5′-end-labeled 650 bp (*Hin*dIII* 13972–*Eco*RI* 14621) and 460 bp (*Hin*dIII* 13038–*Eco*RI* 13507) fragments were obtained as described previously [17]. The 650 bp fragment was digested with *Apa*I to obtain the singly labeled 211 bp (*Hin*dIII* 13972–*Apa*I 14182) and 443 bp (*Apa*I 14179–*Eco*RI* 14621) DNA fragments. The 460 bp fragment was digested with *Sty*I to obtain the singly labeled 118 bp (*Hin*dIII* 13038–*Sty*I 13155) and 348 bp (*Sty*I 13160–*Eco*RI* 13507) fragments. For reference, nucleotide numbering starts with the Bam HI site [18]. An asterisk indicates ^{32}P-labeling.

2.5. Detection of DNA damage caused by GA in the presence of metal ions

The standard reaction mixture contained GA, ^{32}P-5′-end-labeled DNA fragments, 20 μM/base calf thymus DNA and 20 μM metal ions in 200 μl of 10 mM sodium phosphate buffer (pH 7.8) containing 5 μM DTPA. After incubation at 37 °C for 1 h, the DNA fragments were heated at 90 °C in 1 M piperidine for 20 min.

The preferred cleavage sites were determined by direct comparison of the positions of the oligonucleotides with those produced by the chemical reactions of the Maxam–Gilbert procedure [19] using a DNA-sequencing system (LKB 2010 Macrophor, Pharmacia Biotech, Uppsala, Sweden). The relative amounts of oligonucleotides from the treated DNA fragments were measured with a laser densitometer (LKB 2222 UltroScan XL, Pharmacia Biotech).

2.6. Analysis of formation of 8-oxodG in calf thymus DNA by GA in the presence of metal ions

The amounts of 8-oxodG were measured by modified methods of Kasai et al. [20]. Calf thymus DNA (100 μM/base) and 20 μM metal ($CuCl_2$, Fe(III)EDTA or Fe(III)ADP) were incubated with GA, in 200 μl of 4 mM sodium phosphate buffer (pH 7.8) containing 5 μM DTPA for 1 h at 37 °C. After ethanol precipitation, DNA fragments were digested to individual nucleosides with nuclease P1 and CIP, and analyzed with an HPLC-ECD, as described previously [11].

2.7. UV-Vis spectra measurement during autooxidation of GA and PG

UV-Vis spectra of GA and PG were measured with a UV-Vis spectrometer (UV-2500PC, Shimadzu, Kyoto). The reaction mixture contained 2 mM GA or PG and 200 μM $CuCl_2$ or Fe(III)EDTA in 10 mM phosphate buffer (pH 7.8). The spectra of the mixtures were measured repeatedly at 37 °C for the indicated duration.

2.8. Ab initio molecular orbital calculation of GA and PG

Energies of highest occupied molecular orbital (HOMO) of GA and PG were estimated from ab initio molecular orbital (MO) calculation at Hartree–Fock 6-31G* level. The calculations were performed using Spartan 02′ for Windows (Wavefunction Inc., CA) as previously reported [21].

3. Results

3.1. Formation of 8-oxodG in human cultured cells by PG

Fig. 1 compared 8-oxodG formation in HL-60 cells and HP100 cells, which are an H_2O_2-resistant clone of HL-60 cells. The content of 8-oxodG of DNA in HL-60 cells treated with 200 and 500 μM PG was significantly increased in comparison with no treated cells, whereas PG did not significantly increase the amount of 8-oxodG in HP100 cells. Catalase activity of HP100 cells is 18 times higher than that of parent HL-60 cells [22]. These findings suggested that the generation of H_2O_2 plays a critical role in PG-induced DNA damage.

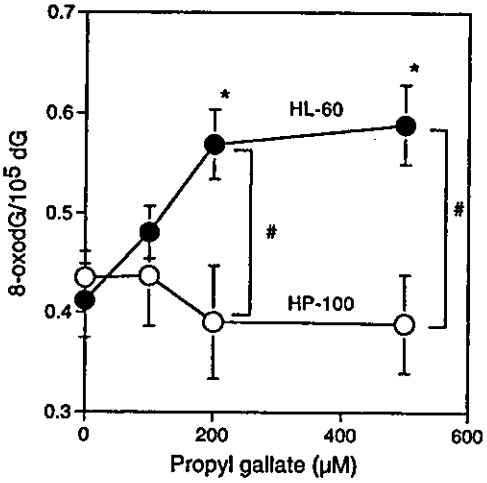

Fig. 1. Comparison of 8-oxodG formation in HL-60 and HP100 cells treated with PG. HL-60 (●) and HP100 (○) cells (10^6 cells/ml) were incubated with PG for 2 h at 37 °C and the DNA was extracted immediately. DNA was digested to nucleosides enzymatically and 8-oxodG content was analyzed by HPLC-ECD, as described in Section 2. Results are expressed as mean ± S.E. of values obtained from six independent experiments. Symbols indicate significant differences compared with control (*: $P < 0.05$) and significant differences between HL-60 and HP100 at the same dose of PG (#: $P < 0.05$) by *t*-test.

3.2. Identification of a product generated from PG treated with esterase

The product generated from PG treated with esterase was analyzed with an HPLC equipped with a photodiode array. The product eluting at 3.0 min showed a maximum absorption at 272 nm (Fig. 2). This product was identified to be GA based on its HPLC elution profile and UV spectral properties. The amounts of GA generated by PG plus esterase were measured with passage of time. When PG was incubated with esterase for 1 and 3 h, 40 and 70% of PG were converted into GA, respectively.

3.3. Damage to ^{32}P-labeled DNA fragments by PG, PG with esterase, and GA in the presence of metal ions

PG induced no or little DNA damage in the presence of metal ions (Fig. 3A). However, when PG

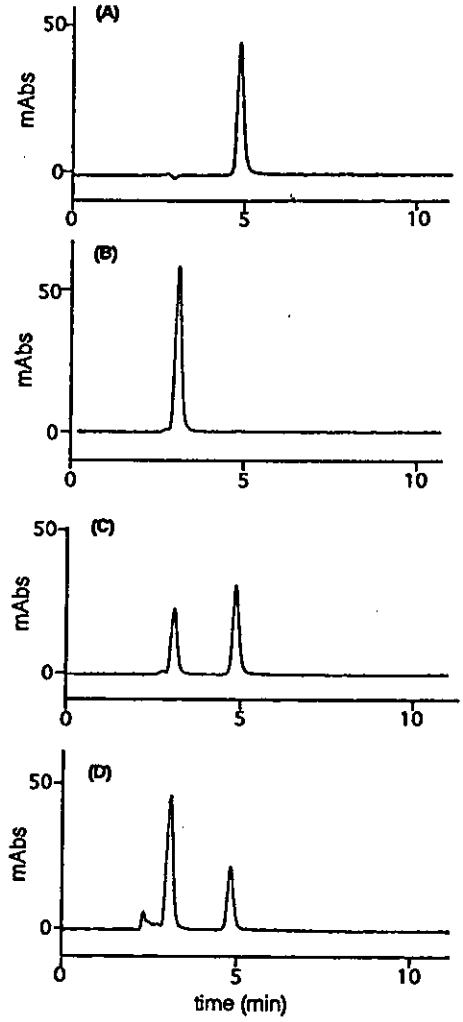

Fig. 2. HPLC chromatograms of PG, GA, and PG treated with esterase. (A) Chromatogram of authentic PG. The mixture containing 100 μM PG in 50 μl of 10 mM sodium phosphate buffer (pH 7.8) containing 5 μM DTPA was analyzed with an HPLC as described in Section 2. (B) Chromatogram of authentic GA. The mixture containing 100 μM GA in 50 μl of 10 mM sodium phosphate buffer (pH 7.8) containing 5 μM DTPA was analyzed with an HPLC. (C) Chromatogram of PG incubated with esterase for 1 h. The mixture containing 100 μM PG in 50 μl of 10 mM sodium phosphate buffer (pH 7.8) containing 5 μM DTPA was incubated with 0.625 U esterase for 1 h at 37 °C and analyzed with an HPLC. (D) Chromatogram of PG incubated with esterase for 3 h. The mixture containing 100 μM PG in 50 μl of 10 mM sodium phosphate buffer (pH 7.8) containing 5 μM DTPA was incubated with 0.625 U esterase for 3 h at 37 °C and analyzed with an HPLC.

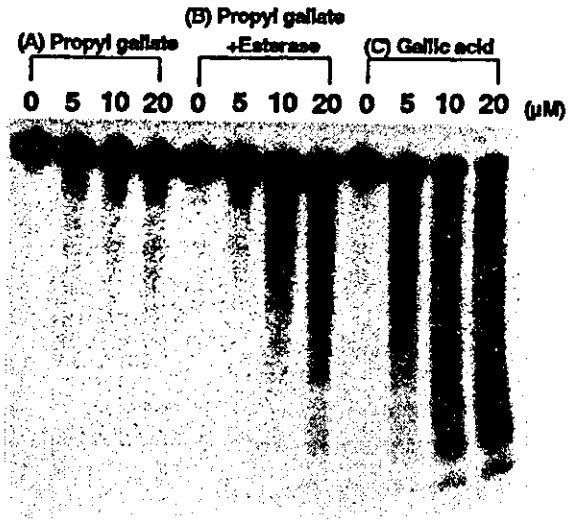

Fig. 3. Damage to ^{32}P-labeled DNA fragments by PG, esterase-treated PG, and GA in the presence of Cu(II). (A) The reaction mixtures containing ^{32}P-5′-end-labeled DNA fragments, 20 μM/base calf thymus DNA, indicated concentrations of PG and 20 μM $CuCl_2$ were incubated for 1 h at 37 °C. (B) The reaction mixtures containing indicated concentrations of PG and 0.625 U esterase in 10 mM sodium phosphate buffer (pH 7.8) containing 5 μM DTPA were incubated for 3 h at 37 °C. After preincubation, ^{32}P-5′-end labeled DNA fragments, 20 μM/base calf thymus DNA and 20 μM $CuCl_2$ were added to the mixtures, followed by the incubation for 1 h at 37 °C. (C) The reaction mixtures containing ^{32}P-5′-end labeled DNA fragments, 20 μM/base calf thymus DNA, indicated concentrations of GA and 20 μM $CuCl_2$ were incubated for 1 h at 37 °C. Subsequently, DNA fragments were treated with 1 M piperidine for 20 min at 90 °C, then electrophoresed on an 8% polyacrylamide/8 M urea gel. The autoradiogram was visualized by exposing an X-ray film to the gel.

was incubated with esterase, DNA damage was observed in the presence of Cu(II) (Fig. 3B). GA also induced DNA damage in a dose-dependent manner in the presence of Cu(II) (Fig. 3C). Piperidine treatment enhanced DNA cleavage by GA, suggesting that GA plus Cu(II) caused not only direct breakage of the deoxyribose phosphate backbone but also base modification (data not shown). Similar results was obtained with GA in the presence of Fe(III)EDTA. Direct breakage and piperidine-sensitive base modification caused by GA plus Cu(II) were stronger than those by GA plus Fe(III)EDTA (data not shown).

3.4. Effects of scavengers and metal chelators on DNA damage induced by GA in the presence of metal ions

In the presence of Fe(III)EDTA, DNA damage induced by GA was inhibited by free hydroxyl radical (•OH) scavengers such as ethanol, mannitol, sodium formate, DMSO and methional (Fig. 4A). Catalase and deferoxamine mesylate, an iron chelating agent, also inhibited the DNA damage (Fig. 4A). SOD did not inhibit the DNA damage (Fig. 4A). These results indicated that •OH, H_2O_2, and iron participated in the Fe(III)EDTA-mediated DNA damage.

In the presence of Cu(II), •OH scavengers showed little or no inhibitory effect on DNA damage by GA (Fig. 4B). However, the DNA damage was inhibited by methional (Fig. 4B), which can scavenge not only •OH but also species with weaker reactivity than •OH [23]. Catalase and bathocuproine, a Cu(I) chelator, inhibited the DNA damage, suggesting the involvement of H_2O_2 and Cu(I) (Fig. 4B). From these results, we speculated that reactive oxygen species such as DNA-copper–hydroperoxo complex participated in the Cu(II)-mediated DNA damage caused by GA.

3.5. Site specificity of DNA cleavage by GA in the presence of metal ions

Fig. 5 shows the patterns of DNA damage induced by GA in the presence of Fe(III)EDTA or Cu(II). The relative intensity of DNA damage was obtained by scanning autoradiogram with a laser densitometer. In the presence of Fe(III)EDTA, GA caused DNA damage at every nucleotide in DNA fragments treated with piperidine (Fig. 5A). In the presence of Cu(II), DNA damage caused by GA occurred frequently at thymine and cytosine with piperidine treatment (Fig. 5B).

3.6. Formation of 8-oxodG in calf thymus DNA by GA in the presence of metal ions

We measured the 8-oxodG content in calf thymus DNA incubated with GA. As shown in Fig. 6, GA increased formation of 8-oxodG in the presence of metal ions. At GA concentrations above 50 μM, Cu(II) led to the formation of 8-oxodG more efficiently than

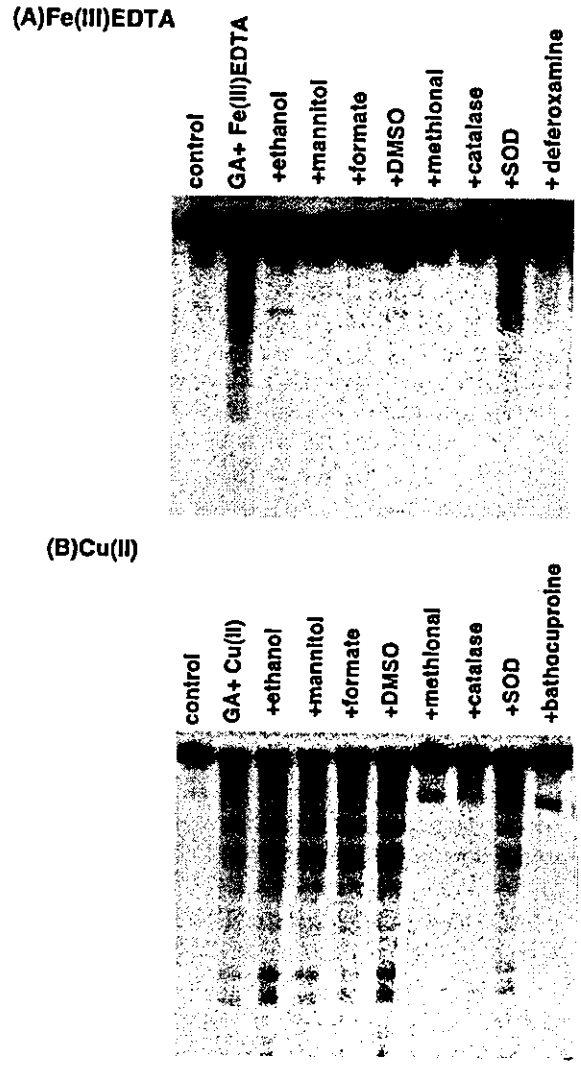

Fig. 4. Effects of scavengers and metal chelators on DNA damage induced by GA in the presence of Cu(II) and Fe(III)EDTA. Reaction mixtures contained the ^{32}P-5′-end-labeled DNA fragments, 20 μM/base calf thymus DNA, 200 μM (A) or 20 μM (B) GA and 20 μM Fe(III)EDTA (A) or $CuCl_2$ (B) in 200 μl of 10 mM sodium phosphate buffer (pH 7.8) containing 5 μM DTPA. The mixtures were incubated for 1 h at 37 °C. DNA fragments were treated with 1 M piperidine for 20 min at 90 °C, then electrophoresed on an 8% polyacrylamide/8 M urea gel. The autoradiogram was visualized by exposing an X-ray film to the gel. The concentration of scavengers and metal chelators was as follows, 0.8 M ethanol, 0.1 M mannitol, 0.1 M sodium formate, 0.8 M DMSO, 0.1 M methional, 30 U catalase, 30 U SOD, 20 μM bathocuproine, and 1 mM deferoxamine.

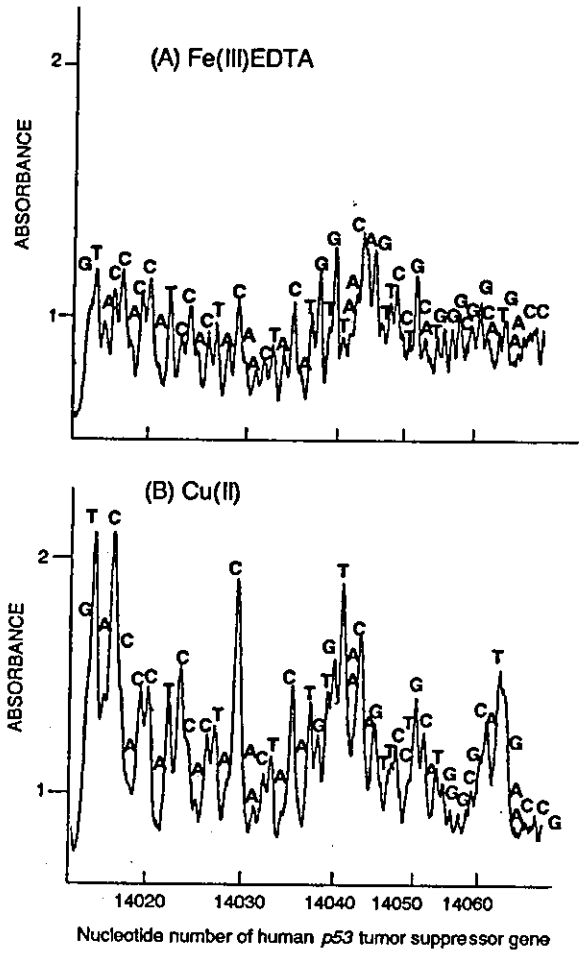

Fig. 5. Site specificity of DNA damage induced by GA in the presence of Cu(II) and Fe(III)EDTA. Reaction mixtures contained the ^{32}P-5′-end-labeled 211 bp DNA fragment (*Hin*dIII* 13972–*Apa*I 14182), 20 μM/base of calf thymus DNA, 200 μM (A) or 20 μM (B) GA and 20 μM Fe(III)EDTA (A) or $CuCl_2$ (B) in 200 μl of 10 mM sodium phosphate buffer (pH 7.8) containing 5 μM DTPA. The mixtures were incubated for 1 h at 37 °C. Following piperidine treatment, the DNA fragments were analyzed as described in Section 2.

Fe(III)EDTA. However, GA led to the formation of 8-oxodG in the presence of Fe(III)EDTA as much as that in the presence of Cu(II) at concentrations below 50 μM. The level of 8-oxodG also increased depending on the concentrations of GA in the presence of Fe(III)ADP. PG did not increase the level of 8-oxodG in the presence of metal ions (data not shown).

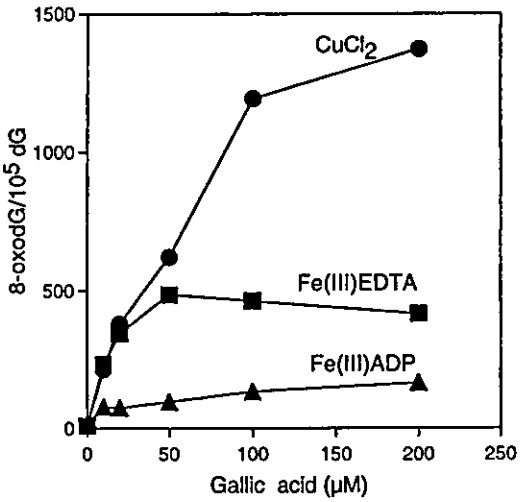

Fig. 6. Formation of 8-oxodG by GA in the presence of metal ions. Reaction mixtures contained 100 μM/base of calf thymus DNA, GA and 20 μM metal ion ($CuCl_2$, Fe(III)EDTA or Fe(III)ADP) was incubated at 37 °C for 1 h. After ethanol precipitation, the DNA was subjected to enzyme digestion and analyzed by HPLC-ECD as described in Section 2.

3.7. UV-Vis spectroscopic study on the autooxidation of GA and PG

The absorption spectra of GA and PG were red-shifted immediately by the addition of $CuCl_2$, possibly due to a complex formation with copper ion. Their absorption bands at ca. 420 nm gradually increased in the presence of Cu(II) (Fig. 7). It has been reported that oxidation of pyrogallol derivatives produce *o*-benzoquinone derivatives, which show characteristic absorption spectrum at ca. 420 nm [24,25]. Therefore, it is reasonably considered that GA and PG, pyrogallol derivatives, produce their corresponding *o*-benzoquinone derivatives via Cu(II)-mediated autooxidation, although a possibility of the formation of the stable one-electron oxidative products cannot be neglected. The spectra changes showed that the oxidation rate of GA is much faster than that of PG. Similar spectra changes were observed in the presence of Fe(III)EDTA (data not shown). Autooxidation of GA mediated by Fe(III)EDTA was faster than that by Cu(II).

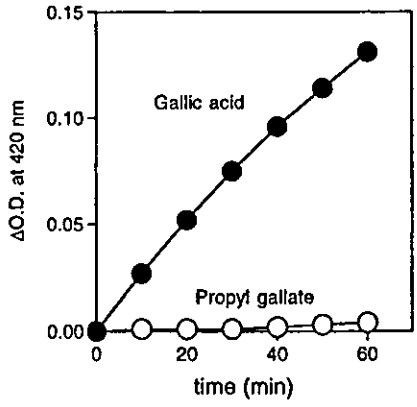

Fig. 7. Increase of absorbance of GA and PG during their autooxidation. Reaction mixture contained 2 mM GA or PG and 200 μM $CuCl_2$ in 10 mM sodium phosphate buffer (pH 7.8) containing 5 μM DTPA. The absorption spectra were measured every 10 min for 60 min with a UV-Vis spectrometer at 37 °C. The increments of absorbance at 420 nm (ΔO.D.) were plotted against the reaction time.

3.8. Calculated energies of the HOMO of GA and PG

The ab initio MO calculation has indicated that the HOMO of these compounds are localized on their phenyl rings. Since pK_a of GA is below 3.4 [26], GA becomes anion form in this experimental condition (pH 7.8). The HOMO energy of anion form of GA (4.71 eV) is smaller than that of PG (8.53 eV). This calculation study suggested that anion form of GA, a hydrolysis product of PG, easily undergo the oxidation rather than the parent PG.

4. Discussion

In this study, we demonstrated that PG significantly increased 8-oxodG formation in HL-60 cells, but did not increased it in HP100 cells. The catalase activity of HP100 cells was 18 times higher than that of HL-60 cells [22]. Therefore, it is suggested that generation of H_2O_2 plays an important role in PG-induced 8-oxodG formation in human cultured cells. The DNA base damage 8-oxodG formation, is a prominent indicator of oxidative stress and has been well-characterized as a premutagenic lesion in mammalian cells. Numerous studies have indicated that the formation of 8-oxodG causes misreplication of DNA that may lead to mutation or cancer [9,10]. It has been reported that guanine to thymine transversion is the most common mispairing-type mutation produced by 8-oxodG in site

specificity assays [9,27]. It is reasonably considered that oxidative DNA damage participates in carcinogenesis induced by PG.

Although PG increased 8-oxodG formation in HL-60 cells, PG itself did not increased the level of 8-oxodG in isolated calf thymus DNA in the presence of metal ions. To clarify the mechanism of cellular DNA damage induced by PG, we investigated formation of 8-oxodG induced by GA in calf thymus DNA. PG is hydrolyzed enzymatically to GA by cellular carboxylesterase. We demonstrated that GA increased the amounts of 8-oxodG in the presence of Cu(II), Fe(III)EDTA, and Fe(III)ADP. From these results, it is considered that GA, produced from PG by esterase, may be involved in oxidative DNA damage in human cultured cell.

Furthermore, we investigated site-specific DNA damage by GA, using ^{32}P-labeled DNA fragments obtained from the human *p53* and *p16* tumor suppressor genes. GA induced DNA damage in the presence of Fe(III) complex or Cu(II). GA caused cleavage uniformly at every nucleotide in the presence of Fe(III)EDTA. A similar pattern was observed in GA induced-DNA damage in the presence of Fe(III)ADP. It is reported that •OH causes DNA cleavage without site specificity [28–31]. In order to confirm what kinds of reactive oxygen species cause oxidative DNA damage, the effects of various scavengers on the Fe(III)EDTA-mediated DNA damage by GA were examined. The inhibitory effects of •OH scavengers, catalase and the iron chelating agent suggested that •OH, H_2O_2, and iron play important roles in the DNA damage. Therefore, we conclude that the Fe(III) complex-mediated DNA damage caused by GA is mainly due to •OH generated via the Fenton reaction.

GA plus Cu(II) induced piperidine-labile site at thymine and cytosine. In addition, using an HPLC-ECD, we also observed the increase of 8-oxodG, which is piperidine-inert site. Thus, GA with Cu(II) should cause oxidative damage at guanine. DNA damage caused by GA plus Cu(II) was inhibited by catalase and bathocuproine, a Cu(I) chelator. Although •OH scavengers showed no or little inhibitory effect on the DNA damage, methional, which can scavenge not only •OH but also species with weaker reactivity than •OH [23], inhibited the DNA damage. From these results, we considered that reactive species such as Cu(I)–hydroperoxo complex partic-

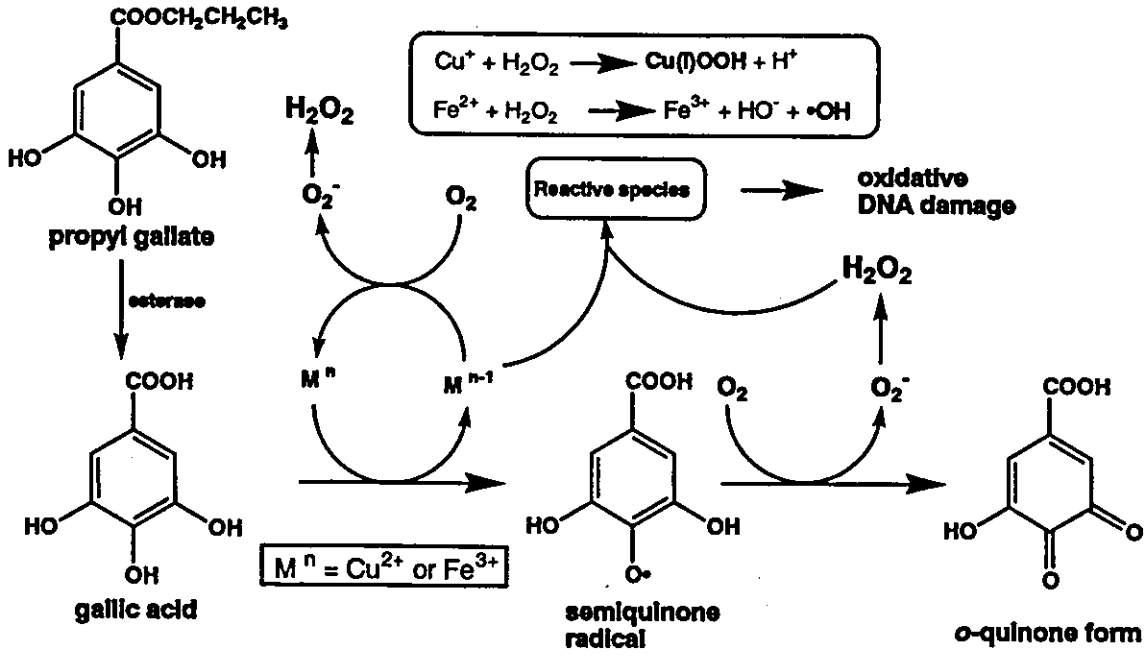

Fig. 8. Possible mechanism of metal-mediated DNA damage induced by GA, a metabolite of PG.

ipate in the Cu(II)-mediated DNA damage by GA. Copper, which occurs in the mammalian cell nucleus, is believed to play a central role in the formation of reactive oxygen species and produce DNA damage leading to carcinogenesis [32].

On the basis of these results, the possible mechanisms of metal-mediated DNA damage induced by GA, a metabolite of PG, are proposed in Fig. 8. Metal-mediated autooxidation of GA generate to the semiquinone radical. In the presence of metal ion (M^n), H_2O_2 was generated by $O_2^{\bullet -}$ dismutation with concomitant reduction of M^n to M^{n-1}. In the presence of Cu(II), GA induced DNA damage by the interaction of Cu(I) and H_2O_2 to form a Cu(I)–hydroperoxo complex such as Cu(I)OOH. Fe(III)EDTA-mediated DNA damage resulting from exposure to GA is caused by $^{\bullet}OH$ generated from the Fenton reaction. $^{\bullet}OH$ is extremely short-lived and travels a very short distance in water [33–35]. This could be one of the reasons that Cu(II)-mediated DNA damage caused by GA was stronger than Fe(III)EDTA-mediated damage, although autooxidation of GA mediated by Fe(III)EDTA was faster than that by Cu(II).

It has been reported that PG can act as carcinogen in several tumor in experimental animals [4,5]. Jacobi et al. [36] reported that PG induced single strand breaks in the presence of Cu(II). However, our study revealed that although PG induced no or little DNA damage in the presence of metal ions, GA efficiently induced DNA damage in the presence of metal ions such as iron and copper under the experimental condition. Absorption spectroscopic studies demonstrated that the autooxidation of GA was markedly faster than that of PG. This observation was supported by MO calculation suggesting that oxidation potential of GA is smaller than that of PG. The experimental and the calculation results lead us to the idea that GA, hydrolysis product of PG, can be easily oxidized than PG, resulting in the enhancement of redox activity to produce reactive oxygen species. Finally, we conclude that GA plays an important role in the express of PG carcinogenicity.

Acknowledgements

This work was supported by Japan Health Foundation, Health Research Foundation, and grants-in-aid for Scientific Research from the Ministry of Education, Science, Sports and Culture of Japan.

References

[1] M.M. King, P.B. McCay, Modulation of tumor incidence and possible mechanisms of inhibition of mammary carcinogenesis by dietary antioxidants, Cancer Res. 43 (1983) 2485–2490.
[2] M. Hirose, A. Masuda, S. Fukushima, N. Ito, Effects of subsequent antioxidant treatment on 7,12-dimethylbenz[a] anthracene-initiated carcinogenesis of the mammary gland, ear duct and forestomach in Sprague–Dawley rats, Carcinogenesis 9 (1988) 101–104.
[3] M. Hirose, H. Yada, K. Hakoi, S. Takahashi, N. Ito, Modification of carcinogenesis by alpha-tocopherol, *t*-butylhydroquinone, propyl gallate and butylated hydroxytoluene in a rat multi-organ carcinogenesis model, Carcinogenesis 14 (1993) 2359–2364.
[4] National Toxicology Program (NTP) Technical Report Carcinogenesis Bioassay of Propyl Gallate (CAS No. 121-79-9) in F344/N Rats and B6C3F1 Mice (Feed Study), NTP TR 240, NTIS# Publication No. 83-180042, 1982.
[5] M. Miyauchi, H. Nakamurak, F. Furukawa, H.Y. Son, A. Nishikawa, M. Hirose, Promoting effects of combined antioxidant and sodium nitrite treatment on forestomach carcinogenesis in rats after initiation with *N*-methyl-*N'*-nitro-*N*-nitrosoguanidine, Cancer Lett. 178 (2002) 19–24.
[6] Y. Nakagawa, K. Nakajima, S. Tayama, P. Moldeus, Metabolism and cytotoxicity of propyl gallate in isolated rat hepatocytes: effects of a thiol reductant and an esterase inhibitor, Mol. Pharmacol. 47 (1995) 1021–1027.
[7] M.P. Rosin, H.F. Stich, Enhancing and inhibiting effects of propyl gallate on carcinogen-induced mutagenesis, J. Environ. Pathol. Toxicol. 4 (1980) 159–167.
[8] S. Tayama, Y. Nakagawa, Cytogenetic effects of propyl gallate in CHO-K1 cells, Mutat. Res. 498 (2001) 117–127.
[9] S. Shibutani, M. Takeshita, A.P. Grollman, Insertion of specific bases during DNA synthesis past the oxidation-damaged base 8-oxodG, Nature 349 (1991) 431–434.
[10] K.C. Cheng, D.S. Cahill, H. Kasai, S. Nishimura, L.A. Loeb, 8-Hydroxyguanine, an abundant form of oxidative DNA damage, causes G–T and A–C substitutions, J. Biol. Chem. 267 (1992) 166–172.
[11] K. Ito, S. Inoue, K. Yamamoto, S. Kawanishi, 8-Hydroxydeoxyguanosine formation at the 5′ site of 5′-GG-3′ sequences in double-stranded DNA by UV radiation with riboflavin, J. Biol. Chem. 268 (1993) 13221–13227.
[12] S. Tada-Oikawa, S. Oikawa, S. Kawanishi, Determination of DNA damage, peroxide generation, Methods Enzymol. 319 (2000) 331–342.
[13] Y. Hiraku, J. Sugimoto, T. Yamaguchi, S. Kawanishi, Oxidative DNA damage induced by aminoacetone, an amino acid metabolite, Arch. Biochem. Biophys. 365 (1999) 62–70.
[14] M. Serrano, G.J. Hannon, D. Beach, A new regulatory motif in cell-cycle control causing specific inhibition of cyclin D/CDK4, Nature 366 (1993) 704–707.

[15] S. Oikawa, K. Murakami, S. Kawanishi, Oxidative damage to cellular and isolated DNA by homocysteine: implications for carcinogenesis, Oncogene 22 (2003) 3530–3538.
[16] P. Chumakov, EMBL Data Library Accession Number X54156, 1990.
[17] N. Yamashita, M. Murata, S. Inoue, Y. Hiraku, T. Yoshinaga, S. Kawanishi, Superoxide formation and DNA damage induced by a fragrant furanone in the presence of copper(II), Mutat. Res. 397 (1998) 191–201.
[18] D.J. Capon, E.Y. Chen, A.D. Levinson, P.H. Seeburg, D.V. Goeddel, Complete nucleotide sequences of the T24 human bladder carcinoma oncogene and its normal homologue, Nature 302 (1983) 33–37.
[19] A.M. Maxam, W. Gilbert, Sequencing end-labeled DNA with base-specific chemical cleavages, Methods Enzymol. 65 (1980) 499–560.
[20] H. Kasai, P.F. Crain, Y. Kuchino, S. Nishimura, A. Ootsuyama, H. Tanooka, Formation of 8-hydroxyguanine moiety in cellular DNA by agents producing oxygen radicals and evidence for its repair, Carcinogenesis 7 (1986) 1849–1851.
[21] K. Hirakawa, M. Yoshida, S. Oikawa, S. Kawanishi, Base oxidation at 5′-site of GG sequence in double-stranded DNA induced by UVA in the presence of xanthone analogues: relationship between the DNA-damaging abilities of photosensitizers and their HOMO energies, Photochem. Photobiol. 77 (2003) 349–355.
[22] I. Kasugai, M. Yamada, High production of catalase in hydrogen peroxide-resistant human leukemia HL-60 cell lines, Leuk. Res. 16 (1992) 173–179.
[23] P.S. Rao, J.M. Luber Jr., J. Milinowicz, P. Lalezari, H.S. Muller, Specificity of oxygen radical scavengers and assessment of free radical scavenger efficiency using luminol enhanced chemiluminesence, Biochem. Biophys. Res. Communi. 150 (1988) 39–44.
[24] W. Bors, C. Michel, K. Stettmaier, Electron paramagnetic resonance studies of radical species of proanthocyanidins and gallate ester, Arch. Biochem. Biophys. 374 (2000) 347–355.
[25] S. Marklund, G. Marklund, Involvement of the superoxide anion radical in the autooxidation of pyrogallol and a convenient assay for superoxide dismutas, Eur. J. Biochem. 47 (1974) 469–479.
[26] K. Polewski, S. Kniat, D. Slawi'nska, Gallic acid, a natural antioxidant, in aqueous and micellar environment: spectroscopic studies, Curr. Top. Biophys. 26 (2002) 217–227.
[27] R.A. Floyd, The role of 8-hydroxyguanine in carcinogenesis, Carcinogenesis 11 (1990) 1447–1450.
[28] R.P. Hertzberg, P.B. Dervan, Cleavage of DNA with methidiumpropyl-EDTA-iron(II): reaction conditions and product analyses, Biochemistry 23 (1984) 3934–3945.
[29] S. Inoue, S. Kawanishi, Hydroxyl radical production and human DNA damage induced by ferric nitrilotriacetate and hydrogen peroxide, Cancer Res. 47 (1987) 6522–6527.
[30] S. Kawanishi, S. Inoue, S. Sano, Mechanism of DNA cleavage induced by sodium chromate(VI) in the presence of hydrogen peroxide, J. Biol. Chem. 261 (1986) 5952–5958.
[31] D.W. Celander, T.R. Cech, Iron(II)-ethylenediaminetetraacetic acid catalyzed cleavage of RNA and DNA oligonucleotides: similar reactivity toward single- and double-stranded forms, Biochemistry 29 (1990) 1355–1361.
[32] T. Theophanides, J. Anastassopoulou, Copper and carcinogenesis, Crit. Rev. Oncol. Hematol. 42 (2002) 57–64.
[33] S. Oikawa, S. Kawanishi, Distinct mechanisms of site-specific DNA damage induced by endogenous reductants in the presence of iron(III) and copper(II), Biochim. Biophys. Acta. 1399 (1998) 19–30.
[34] J. Tchou, A.P. Grollman, Repair of DNA containing the oxidatively-damaged base, 8-oxoguanine, Mutat. Res. 299 (1993) 277–287.
[35] W.A. Pryor, Oxy-radicals and related species: their formation, lifetimes, and reactions, Annu. Rev. Physiol. 48 (1986) 657–667.
[36] H. Jacobi, B. Eicke, I. Witte, DNA strand break induction and enhanced cytotoxicity of propyl gallate in the presence of copper(II), Free Radic. Biol. Med. 24 (1998) 972–978.

Available online at www.sciencedirect.com
SCIENCE DIRECT®
Biochemical and Biophysical Research Communications 316 (2004) 123–128
BBRC
www.elsevier.com/locate/ybbrc

Oxidative DNA damage induced by nitrotyrosine, a biomarker of inflammation☆

Mariko Murata and Shosuke Kawanishi*

Department of Environmental and Molecular Medicine, Mie University School of Medicine, Edobashi, Tsu, Mie 514-8507, Japan

Received 19 December 2003

Abstract

Inflammation has been postulated as a risk factor for several cancers. 3-Nitrotyrosine is a biochemical marker for inflammation. We investigated the ability of nitrotyrosine and nitrotyrosine-containing peptides (nitroY-peptide) to induce DNA damage by the experiments using ^{32}P-labeled DNA fragments obtained from the human *p53* tumor suppressor gene and an HPLC-electrochemical detector. Nitrotyrosine and nitroY-peptide caused Cu(II)-dependent DNA damage in the presence of P450 reductase, which is considered to yield nitroreduction. Catalase inhibited DNA damage, suggesting the involvement of H_2O_2. Nitrotyrosine and nitroY-peptide increased 8-oxo-7,8-dihydro-2′-deoxyguanosine (8-oxodG) formation, an indicator of oxidative DNA damage. Nitrotyrosine-containing peptides of histone induced 8-oxodG formation more efficiently than free nitrotyrosine. We propose the possibility that nitrotyrosine-induced H_2O_2 formation and DNA damage contribute to inflammation-associated carcinogenesis.

Keywords: Nitrotyrosine; Oxidative DNA damage; P450 reductase; Copper; Hydrogen peroxide; Inflammation; Carcinogenesis

Inflammation has been postulated as a risk factor for several cancers [1–5]. Inflammation and infection activate a variety of inflammatory cells, which produce nitric oxide (NO) and superoxide ($O_2^{\cdot-}$), yielding peroxynitrite ($ONOO^-$), and other types of reactive nitrogen species (RNS) [6,7]. The reaction of RNS with protein-bound tyrosine residues causes nitrotyrosine formation in inflammatory and infected tissues. Many studies revealed the presence of 3-nitrotyrosine in human tissues and fluids due to inflammation and infectious diseases [8–11]. Nitrotyrosine serves as a biochemical marker for inflammation. Increases of protein tyrosine nitration were observed in cancer sites [12,13]. Interestingly, a recent study has suggested that histones are the most prominent nitrated proteins in the Mutatec tumor tissue exposed to NO [14]. Irie et al. [15] have demonstrated that histone is a substrate for "denitrase" that removes the nitro group of nitrotyrosine in proteins. The existence of a repair mechanism for nitrated tyrosine in histone has led us to an idea that nitrotyrosine may have deleterious effects on biological system. There arises a possibility that nitrotyrosine can be involved in DNA damage, which may participate in inflammation-associated carcinogenesis.

We investigated the ability of nitrotyrosine and nitrotyrosine-containing peptides of histone to induce DNA damage using ^{32}P-labeled DNA fragments obtained from the human *p53* and *p16* tumor suppressor genes. We also analyzed 8-oxo-7,8-dihydro-2′-deoxyguanosine (8-oxodG) formation in calf thymus DNA with an electrochemical detector coupled to an HPLC (HPLC-ECD), as an indicator of oxidative DNA damage.

Materials and methods

Materials. Restriction enzymes (*Eco*RI, *Mro*I, and *Apa*I) and calf intestine phosphatase were purchased from Boehringer–Mannheim (Germany). Restriction enzymes (*Hin*dIII and *Ava*I) and T_4 polynucleotide

☆ *Abbreviations:* nitroY-peptide, nitrotyrosine-containing peptide; RNS, reactive nitrogen species; 8-oxodG, 8-oxo-7,8-dihydro-2′-deoxyguanosine (and also known as 8-hydroxy-2′-deoxyguanosine); DTPA, diethylenetriamine-*N*,*N*,*N*′,*N*″,*N*″-pentaacetic acid; HPLC-ECD, high performance liquid chromatography coupled with an electrochemical detector; NADPH, β-nicotinamide adenine dinucleotide phosphate (reduced form); P450 reductase, NADPH-cytochrome P450 reductase; SOD, superoxide dismutase.

* Corresponding author. Fax: +81-59-231-5011.
E-mail address: kawanisi@doc.medic.mie-u.ac.jp (S. Kawanishi).

0006-291X/$ - see front matter © 2004 Elsevier Inc. All rights reserved.
doi:10.1016/j.bbrc.2004.02.022

kinase were purchased from New England Biolabs. [γ-^{32}P]ATP (222 TBq/mmol) was from New England Nuclear. Superoxide dismutase (SOD, 3000 U/mg from bovine erythrocytes) and catalase (45,000 U/mg from bovine liver) were from Sigma Chemical. Nitrotyrosine-containing peptides (nitroY-peptide) were supplied by Sawady Technology (Tokyo, Japan; nitroY1-peptide) and Nihon Sigma Genosys Biotechnologies (Hokkaido, Japan; nitroY3-peptide). The amino acid sequences of nitrated tyrosine residue on histone were from reference [14] that identified them in tumor tissue by mass spectrometry as follows; nitroY1-peptide; nitroY-R-P-G-T-V-A-L-R and nitroY3-peptide; E-S-nitroY-S-V-nitroY-V-nitroY-K. NADPH, $NADP^+$, acrylamide, bisacrylamide, and piperidine were obtained from Wako Pure Chemical Industries (Osaka, Japan). NADPH-cytochrome P450 reductase (P450 reductase) from rat microsome was a kind gift from Dr. Y. Kumagai (Tsukuba University). Ethanol and $CuCl_2$ were from Nakalai Tesque (Kyoto, Japan). Nuclease P_1 was from Yamasa Shoyu (Chiba, Japan). Bathocuproinedisulfonic acid was from Dojin Chemicals (Kumamoto, Japan).

Preparation of ^{32}P-5′-end-labeled DNA fragments. DNA fragments obtained from the human *p53* tumor suppressor gene [16] containing exons were prepared, as described previously [17]. The 5′-end-labeled 650-bp fragment (*Hin*dIII*13972–*Eco*RI*14621) was obtained by dephosphorylation with calf intestine phosphatase and rephosphorylation with [γ-^{32}P]ATP and T_4 polynucleotide kinase (*, ^{32}P-labeled). The 650-bp fragment was further digested with *Apa*I to obtain a singly labeled 443-bp fragment (*Apa*I 14179–*Eco*RI*14621) and a 211-bp fragment (*Hin*dIII*13972–*Apa*I 14182). DNA fragment was also obtained from the human *p16* tumor suppressor gene [18]. The 5′ end-labeled 490-bp fragment (*Eco*RI*5841–*Eco*RI*6330) containing exon 1 of the human *p16* tumor suppressor gene was obtained by pGEM-T Easy Vector (Promega). The 490-bp fragment was further digested with *Mro*I to obtain a singly labeled 328-bp fragment (*Eco*RI*5841–*Mro*I 6168) and a 158-bp fragment (*Mro*I 6173–*Eco*RI*6330) as described previously [19].

Detection of DNA damage by nitrotyrosine. The standard reaction mixtures (in a microtube; 1.5 mL; Eppendorf) containing nitrotyrosine, 100 μM NADPH, and P450 reductase in 20 mM potassium phosphate buffer (pH 7.4) were pre-incubated at 25 °C for 30 min. After pre-incubation, ^{32}P-5′-end-labeled DNA fragments, calf thymus DNA (20 μM/base), and 20 μM $CuCl_2$ were added to the mixtures (total 200 μL), followed by the incubation at 37 °C for 1 h. Then, the DNA fragments were treated in 10% (v/v) piperidine at 90 °C for 20 min, or treated with 6 U Fpg protein in 21 μL of reaction buffer (10 mM Hepes–KOH (pH 7.4), 100 mM KCl, 10 mM EDTA, and 0.1 mg/ml BSA) at 37 °C for 2 h. The treated DNA was electrophoresed on an 8% polyacrylamide/8 M urea gel. The autoradiogram was obtained by exposing X-ray film to the gel [19].

The preferred cleavage sites were determined by direct comparison of the positions of the oligonucleotides with those produced by the chemical reactions of the Maxam–Gilbert procedure [20] using a DNA-sequencing system (LKB 2010 Macrophor). The relative amounts of oligonucleotides from the treated DNA fragments were measured with a laser densitometer (LKB 2222 UltroScan XL).

Analysis of 8-oxodG formation in calf thymus DNA by nitrotyrosine. The standard reaction mixture (in a microtube; 1.5 mL; Eppendorf) containing nitrotyrosine, 100 μM NADPH, and P450 reductase in 20 mM potassium phosphate buffer (pH 7.4) were pre-incubated at 25 °C for 30 min. After pre-incubation, calf thymus DNA (100 μM/base) and 20 μM $CuCl_2$ were added, and then incubated at 37 °C for 1 h. After ethanol precipitation, DNA was digested to the nucleosides with nuclease P_1 and calf intestine phosphatase, and analyzed by an HPLC-ECD, as described previously [21].

Measurement of $NADP^+$ amount. The standard reaction mixtures (in a microtube; 1.5 mL; Eppendorf) containing nitrotyrosine, 100 μM NADPH and P450 reductase in 20 mM potassium phosphate buffer (pH 7.4) were pre-incubated at 25 °C for 30 min, followed by incubation at 37 °C for 1 h. $NADP^+$ amount was analyzed by HPLC with a Shimadzu photodiode array UV detector (SPD-M10A, Kyoto, Japan) at 260 nm with Wako Pure Chemical ODS (46 mm × 150 mm) in mobile phase containing 2% methanol and 100 mM potassium phosphate buffer (pH 6) at flow rate 1 mL/min.

Results

Damage to ^{32}P-labeled DNA fragments by nitrotyrosine in the presence of P450 reductase, NADPH, and Cu(II)

Free nitrotyrosine and nitrotyrosine-peptides of histone caused Cu(II)-mediated DNA damage when

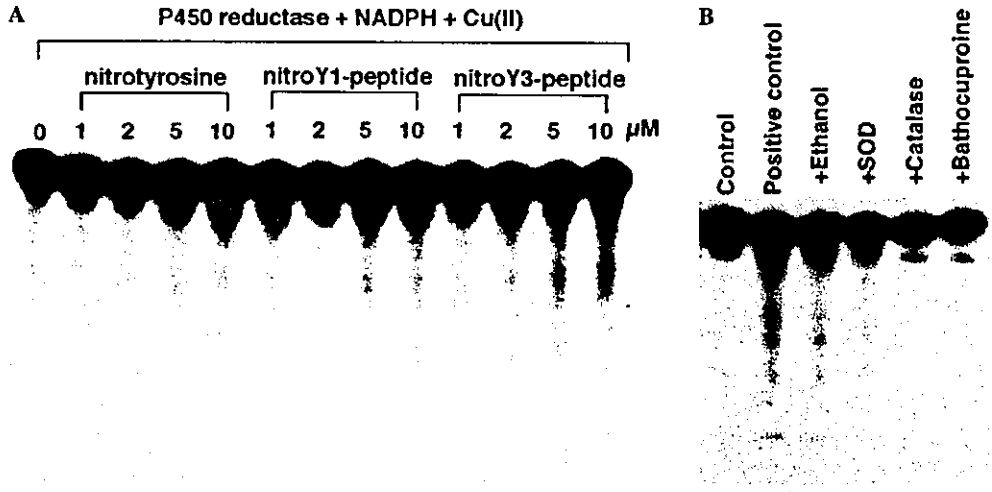

Fig. 1. Autoradiograms of ^{32}P-labeled DNA fragments incubated with free nitrotyrosine and nitroY-peptides in the presence of P450 reductase, NADPH, and Cu(II). (A) The reaction mixtures containing indicated concentrations of nitrotyrosine or nitroY-peptide, 100 μM NADPH, and 2.1 μg/mL P450 reductase in 20 mM potassium phosphate buffer (pH 7.4) were pre-incubated at 25 °C for 30 min. After pre-incubation, ^{32}P-5′-end-labeled 158-bp DNA fragments, calf thymus DNA (20 μM/base), and 20 μM $CuCl_2$ were added to the mixtures (total 200 μL), followed by the incubation at 37 °C for 1 h. (B) Scavengers were added after pre-incubation of 10 μM nitroY3-peptide as follows: 5% (v/v) ethanol; 30 U SOD; 30 U catalase; 50 μM bathocuproine. After the incubation, the DNA fragments were treated with hot piperidine and electrophoresed on an 8% polyacrylamide/8 M urea gel. The autoradiogram was obtained by exposing X-ray film to the gel.

they were treated with P450 reductase (Fig. 1A). Without P450 reductase, free nitrotyrosine and nitroY-peptides caused no DNA damage even in the presence of Cu(II) (data not shown). In the absence of Cu(II), DNA damage was not observed. Free nitrotyrosine induced slight DNA damage. NitroY-peptides damaged DNA more efficiently than free nitrotyrosine. The peptide containing three nitrotyrosine residues (nitroY3-peptide) induced DNA damage stronger than that containing one nitrotyrosine (nitroY1-peptide). The amount of oligonucleotides was increased by piperidine treatment, suggesting the involvement of base modification/liberation (data not shown).

Effects of scavengers and bathocuproine on DNA damage induced by nitrotyrosine

Fig. 1B shows the effects of scavengers and bathocuproine, a Cu(I)-specific chelator, on DNA damage induced by P450 reductase-treated nitroY3-peptide in the presence of Cu(II). Catalase and bathocuproine inhibited DNA damage, suggesting the involvement of hydrogen peroxide (H_2O_2) and Cu(I). Ethanol, a typical free hydroxyl radical (·OH) scavenger, did not attenuate DNA damage. SOD partly inhibited DNA damage. Similar results were obtained with nitroY1-peptide (data not shown).

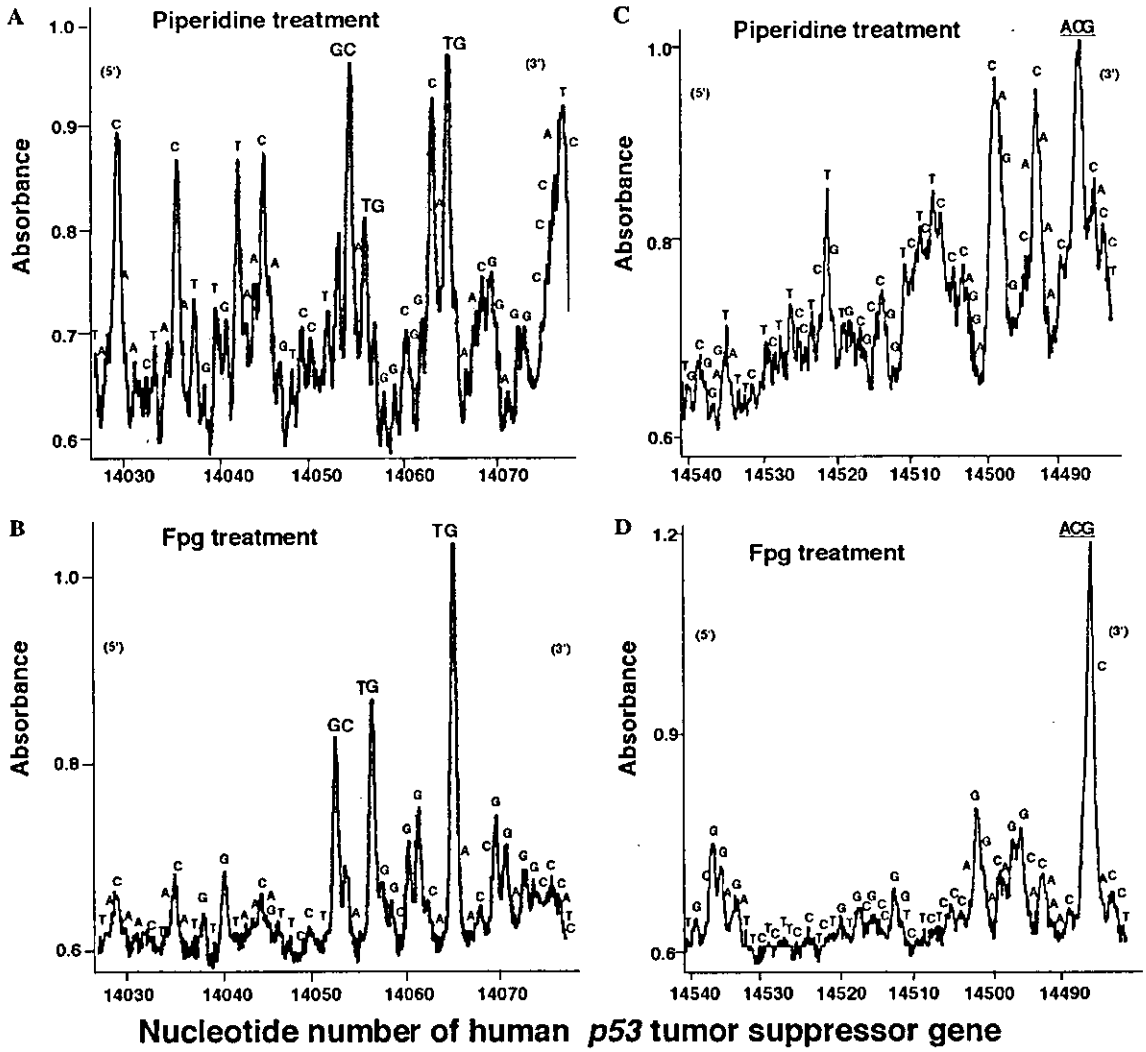

Fig. 2. Site specificity of Cu(II)-mediated DNA cleavage induced by nitroY3-peptide in the presence of P450 reductase. The reaction mixtures containing 10 μM nitroY3-peptide, 100 μM NADPH, and 2.1 μg/mL P450 reductase in 20 mM potassium phosphate buffer (pH 7.4) were pre-incubated at 25 °C for 30 min. After pre-incubation, ^{32}P-5′-end-labeled 211-bp (A,B) or 443-bp (C,D) DNA fragments, calf thymus DNA (20 μM/base), and 20 μM $CuCl_2$ were added to the mixtures. Reaction mixtures were incubated at 37 °C for 1 h, followed by hot piperidine (A,C) and Fpg treatment (B,D). DNA fragments were electrophoresed on an 8% polyacrylamide/8 M urea gel using a DNA-sequencing system and the autoradiogram was obtained by exposing X-ray film to the gel. The relative amounts of oligonucleotide were measured by scanning the autoradiogram with a laser densitometer (LKB 2222 UltroScan XL). The horizontal axis shows the nucleotide number of the human *p53* tumor suppressor gene and underscoring shows the complementary sequence to codon 273 (nucleotide numbers 14486–14488).

Site specificity of DNA cleavage by nitrotyrosine

An autoradiogram was obtained and scanned with a laser densitometer to measure relative intensity of DNA cleavage in the human *p53* tumor suppressor gene (Fig. 2). P450 reductase-treated nitroY-peptide induced piperidine-labile sites relatively at thymine and cytosine residues in the presence of Cu(II) (Figs. 2A and C). With Fpg treatment, DNA cleavage occurred mainly at guanine residues (Figs. 2B and D). Collectively, damage at neighboring guanine and pyrimidine residues such as 5′-TG-3′ and 5′-GC-3′ sites was observed (Figs. 2A and B), suggesting that double-base lesion occurred. NitroY-peptides caused piperidine-labile and Fpg-sensitive lesions at CG in the 5′-ACG-3′ sequence, a well-known hotspot of the *p53* gene [22] (Figs. 2C and D).

Formation of 8-oxodG in calf thymus DNA by nitrotyrosine

Using an HPLC-ECD, we measured 8-oxodG content in calf thymus DNA treated with nitrotyrosine after P450 reductase treatment (Fig. 3). NitroY3-peptide increased the amount of 8-oxodG up to 2 μM and then decreased gradually. Significant increases ($p < 0.01$) were observed in all conditions treated with 1 μM and higher concentrations of nitroY3-peptide. NitroY1-peptide induced the increase of 8-oxodG formation with increasing its concentration (1 μM; $p < 0.05$, 2 μM and higher; $p < 0.01$). Free nitrotyrosine induced the increase of 8-oxodG formation significantly at 10 μM ($p < 0.05$). Nitrotyrosine residue-containing histone-peptides induced 8-oxodG formation much more efficiently than free nitrotyrosine.

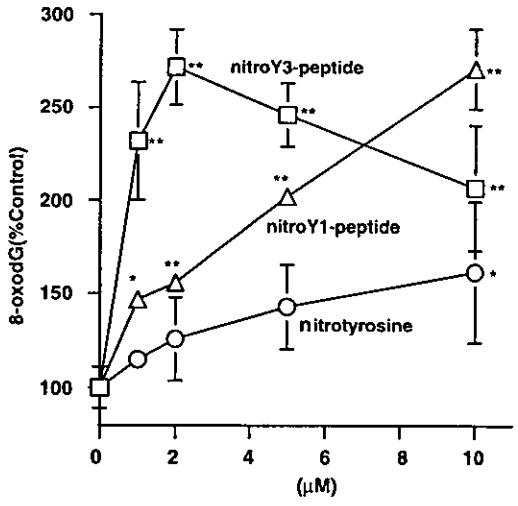

Fig. 3. Cu(II)-mediated formation of 8-oxodG in calf thymus DNA by nitrotyrosine and nitroY-peptides in the presence of P450 reductase. The reaction mixtures containing nitrotyrosine or nitroY-peptides, 100 μM NADPH, and 2.1 μg/mL P450 reductase in 20 mM potassium phosphate buffer (pH 7.4) were pre-incubated at 25 °C for 30 min. After pre-incubation, DNA fragments (100 μM/base) from calf thymus and 20 μM $CuCl_2$ were added and then incubated at 37 °C for 1 h. After ethanol precipitation, DNA was enzymatically digested to the nucleosides and analyzed by an HPLC-ECD. Results are expressed as means (control; 100%) and SEM of values obtained from three independent experiments. Asterisks indicate significant difference compared with control by Student's *t* test (*$p < 0.05$, **$p < 0.01$).

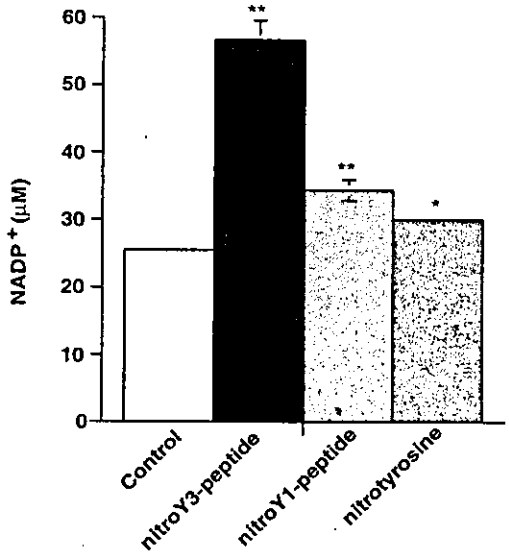

Fig. 4. Production of $NADP^+$ through reaction of nitrotyrosines and P450 reductase. The reaction mixtures containing 10 μM nitrotyrosine or nitroY-peptides, 100 μM NADPH, and 2.1 μg/mL P450 reductase in 20 mM potassium phosphate buffer (pH 7.4) were pre-incubated at 25 °C for 30 min, followed by incubation at 37 °C for 1 h. $NADP^+$ amount was analyzed by HPLC with photodiode array UV detector (260 nm). Results are expressed as means and SEM of values obtained from three independent experiments. Asterisks indicate significant difference compared with control (*$p < 0.05$, **$p < 0.01$) by Student's *t* test.

NADPH oxidation by nitrotyrosine in the presence of P450 reductase

NADPH oxidation to $NADP^+$ was analyzed by HPLC with photodiode array (Fig. 4). Free nitrotyrosine and nitroY-peptides significantly induced $NADP^+$ formation compared with control ($p < 0.05$ and $p < 0.01$, respectively). The amounts of $NADP^+$ by nitroY3-peptide and nitroY1-peptide were significantly higher than that of free nitrotyrosine ($p < 0.01$).

Discussion

The present study has demonstrated that nitrotyrosine and nitroY-peptides of histone have an ability to cause Cu(II)-mediated DNA damage via the activation with P450 reductase. Inhibitory effects of catalase and bathocuproine suggested that H_2O_2 and Cu(I) were required for DNA damage. A possible mechanism of

oxidative DNA damage induced by enzymatically activated nitrotyrosine can be speculated as accounting for most of the observations and references as follows. P450 reductase converts nitrotyrosine to corresponding nitro radical anion in the presence of NADPH via one-electron reduction [23,24]. The nitro radical anion reacts with O_2, followed by production of $O_2^{\cdot-}$ [25] and the consequent oxidation to the parent nitrotyrosine. Alternatively, there is a possibility that further nitroreduction by P450 reductase contributes to the generation of nitroso and/or *N*-hydroxy forms [26]. Any of reduced derivatives such as nitro radical anion, nitroso, and *N*-hydroxy forms may be oxidized again to yield redox cycle with generation of $O_2^{\cdot-}$. Subsequently, the generation of H_2O_2 by $O_2^{\cdot-}$ dismutation and reduction of Cu(II) to Cu(I) concomitantly occur. H_2O_2 reacts with Cu(I) to form a metal–oxygen complex such as Cu(I)-hydroperoxide causing DNA damage. This idea is supported by the observations that a typical free ·OH scavenger, ethanol, did not offer DNA protection. The complex DNA–Cu(I)–hydroperoxide may be considered to be a bound hydroxyl radical, which can release ·OH causing DNA damage. The ·OH released from the bound hydroxyl radical may immediately attack an adjacent constituent of DNA before it is scavenged by free ·OH scavengers [27]. NitroY-peptides damaged DNA more efficiently than free nitrotyrosine did. Relevantly, Krainev et al. [24] showed that nitrotyrosine residue within leucine enkephalin pentapeptide (Tyr–Gly–Gly–Phe–Leu) had a higher affinity for enzymatic reduction with higher production of $O_2^{\cdot-}$ than does free nitrotyrosine. We assessed the efficacy of redox cycling reaction by measuring $NADP^+$ as NADPH oxidation. The result also supported the idea that nitroY-peptides are more easily reduced by NADPH-P450 reductase than free nitrotyrosine. This can reasonably account for different DNA damaging potentials of free nitrotyrosine and nitrotyrosine-containing peptides.

It is considered that tyrosine plays a role in interactions of DNA-binding proteins and histones with DNA [28], probably through the close proximity of thymine and tyrosine in chromatin. Relevantly, Altman et al. [29] provided evidence for the formation of DNA–protein crosslinks between thymine and tyrosine in chromatin when cultured mannalian cells were treated with metal ions. When the tyrosine residues in histone are nitrated, reactive species derived from nitrotyrosine residue will immediately attack DNA. $ONOO^-$ is a potent DNA oxidizing agent [30], but it is very short-lived. On the other hand, nitrotyrosine has a long half-life in vivo. Nitrated proteins were detected for at least 24 h in rat skin singly exposed to $ONOO^-$ [31]. We have shown that enzymatically activated nitrotyrosine in histone peptide induced oxidative DNA damage in the presence of Cu(II). Abundant RNS are generated in inflammatory and infected tissues, and histone proteins are nitrated especially at tyrosine residues [14]. Most of nitrotyrosine in histone will be repaired by "denitrase" [15]. If nitrotyrosine residues still remain in histone, they may cause DNA damage in the presence of P450 reductase. This assumption is supported by the observation that P450 reductase exists in the nuclear fraction [32] although the amount of P450 reductase in nuclear fraction is smaller than that in cytosolic fraction. On the other hand, nitrotyrosine may be more easily catalyzed to reactive species by P450 reductase in cytosolic fraction. Therefore, both nitrotyrosines in cytosol and in nuclear histone may participate in DNA damage. In addition to the fact that nitrotyrosine is a marker for inflammation, we propose the possibility that nitrotyrosine-induced H_2O_2 formation and subsequent DNA damage contribute to inflammation-associated carcinogenesis.

Acknowledgment

This work was supported by a Grant-in-Aid from the Ministry of Education, Science, Sports and Culture of Japan.

References

[1] H. Ohshima, Genetic and epigenetic damage induced by reactive nitrogen species: implications in carcinogenesis, Toxicol. Lett. 140–141 (2003) 99–104.
[2] H. Ohshima, M. Tatemichi, T. Sawa, Chemical basis of inflammation-induced carcinogenesis, Arch. Biochem. Biophys. 417 (2003) 3–11.
[3] H. Wiseman, B. Halliwell, Damage to DNA by reactive oxygen and nitrogen species: role in inflammatory disease and progression to cancer, Biochem. J. 313 (1996) 17–29.
[4] S. Kawanishi, Y. Hiraku, M. Murata, S. Oikawa, The role of metals in site-specific DNA damage with reference to carcinogenesis, Free Radic. Biol. Med. 32 (2002) 822–832.
[5] S. Kawanishi, S. Inoue, S. Oikawa, N. Yamashita, S. Toyokuni, M. Kawanishi, K. Nishino, Oxidative DNA damage in cultured cells and rat lungs by carcinogenic nickel compounds, Free Radic. Biol. Med. 31 (2001) 108–116.
[6] H. Ischiropoulos, Biological selectivity and functional aspects of protein tyrosine nitration, Biochem. Biophys. Res. Commun. 305 (2003) 776–783.
[7] J.P. Eiserich, M. Hristova, C.E. Cross, A.D. Jones, B.A. Freeman, B. Halliwell, A. van der Vliet, Formation of nitric oxide-derived inflammatory oxidants by myeloperoxidase in neutrophils, Nature 391 (1998) 393–397.
[8] A. van der Vliet, J.P. Eiserich, H. Kaur, C.E. Cross, B. Halliwell, Nitrotyrosine as biomarker for reactive nitrogen species, Methods Enzymol. 269 (1996) 175–184.
[9] H. Ischiropoulos, Biological tyrosine nitration: a pathophysiological function of nitric oxide and reactive oxygen species, Arch. Biochem. Biophys. 356 (1998) 1–11.
[10] M.K. Shigenaga, H.H. Lee, B.C. Blount, S. Christen, E.T. Shigeno, H. Yip, B.N. Ames, Inflammation and NOx-induced nitration: assay for 3-nitrotyrosine by HPLC with electrochemical detection, Proc. Natl. Acad. Sci. USA 94 (1997) 3211–3216.

[11] L. Viera, Y.Z. Ye, A.G. Estévez, J.S. Beckman, Immunohistochemical methods to detect nitrotyrosine, Methods Enzymol. 301 (1999) 373–381.
[12] A. Ehsan, F. Sommer, A. Schmidt, T. Klotz, J. Koslowski, S. Niggemann, G. Jacobs, U. Engelmann, K. Addicks, W. Bloch, Nitric oxide pathways in human bladder carcinoma. The distribution of nitric oxide synthases, soluble guanylyl cyclase, cyclic guanosine monophosphate, and nitrotyrosine, Cancer 95 (2002) 2293–2301.
[13] A. Patel, C. Fenton, R. Terrell, P.A. Powers, C. Dinauer, R.M. Tuttle, G.L. Francis, Nitrotyrosine, inducible nitric oxide synthase (iNOS), and endothelial nitric oxide synthase (eNOS) are increased in thyroid tumors from children and adolescents, J. Endocrinol. Invest. 25 (2002) 675–683.
[14] A.S. Haqqani, J.F. Kelly, H.C. Birnboim, Selective nitration of histone tyrosine residues in vivo in mutatect tumors, J. Biol. Chem. 277 (2002) 3614–3621.
[15] Y. Irie, M. Saeki, Y. Kamisaki, E. Martin, F. Murad, Histone H1.2 is a substrate for denitrase, an activity that reduces nitrotyrosine immunoreactivity in proteins, Proc. Natl. Acad. Sci. USA 94 (2003) 5634–5639.
[16] P. Chumakov, EMBL Data Library, Accession No. X54156 (1990).
[17] M. Murata, S. Kawanishi, Oxidative DNA damage by vitamin A and its derivative via superoxide generation, J. Biol. Chem. 275 (2000) 2003–2008.
[18] M. Serrano, G.J. Hannon, D.A. Beach, A new regulatory motif in cell-cycle control causing specific inhibition of cyclin D/CDK4, Nature 366 (1993) 704–707.
[19] S. Oikawa, I. Hirosawa, K. Hirakawa, S. Kawanishi, Site specificity and mechanism of oxidative DNA damage induced by carcinogenic catechol, Carcinogenesis 22 (2001) 1239–1245.
[20] A.M. Maxam, W. Gilbert, Sequencing end-labeled DNA with base-specific chemical cleavages, Methods Enzymol. 65 (1980) 499–560.
[21] K. Ito, S. Inoue, K. Yamamoto, S. Kawanishi, 8-Hydroxydeoxyguanosine formation at the 5′ site of 5′-GG-3′ sequences in double-stranded DNA by UV radiation with riboflavin, J. Biol. Chem. 268 (1993) 13221–13227.
[22] A.J. Levine, J. Momand, C.A. Finlay, The p53 tumor suppressor gene, Nature 351 (1991) 453–456.
[23] T. Akaike, S. Okamoto, T. Sawa, J. Yoshitake, F. Tamura, K. Ichimori, K. Miyazaki, K. Sasamoto, H. Maeda, 8-Nitroguanosine formation in viral pneumonia and its implication for pathogenesis, Proc. Natl. Acad. Sci. USA 100 (2003) 685–690.
[24] A.G. Krainev, T.D. Williams, D.J. Bigelow, Enzymatic reduction of 3-nitrotyrosine generates superoxide, Chem. Res. Toxicol. 11 (1998) 495–502.
[25] M. Murata, M. Kobayashi, S. Kawanishi, Nonenzymatic reduction of nitro derivative of a heterocyclic amine IQ by NADH and Cu(II) leads to oxidative DNA damage, Biochemistry 38 (1999) 7624–7629.
[26] V.M. Arlt, H. Glatt, E. Muckel, U. Pabel, B.L. Sorg, A. Seidel, H. Frank, H.H. Schmeiser, D.H. Phillips, Activation of 3-nitrobenzanthrone and its metabolites by human acetyltransferases, sulfotransferases and cytochrome P450 expressed in Chinese hamster V79 cells, Int. J. Cancer 105 (2003) 583–592.
[27] M. Dizdaroglu, G. Rao, B. Halliwell, E. Gajewski, Damage to the DNA bases in mammalian chromatin by hydrogen peroxide in the presence of ferric and cupric ions, Arch. Biochem. Biophys. 285 (1991) 317–324.
[28] A. Zweidler, Role of individual histone tyrosines in the formation of the nucleosome complex, Biochemistry 31 (1992) 9205–9211.
[29] S.A. Altman, T.H. Zastawny, L. Randers-Eichhorn, M.A. Cacciuttolo, S.A. Akman, M. Dizdaroglu, G. Rao, Formation of DNA–protein cross-links in cultured mammalian cells upon treatment with iron ions, Free Radic. Biol. Med. 19 (1995) 897–902.
[30] S. Inoue, S. Kawanishi, Oxidative DNA damage induced by simultaneous generation of nitric oxide and superoxide, FEBS Lett. 371 (1995) 86–88.
[31] S.A.B. Greenacre, P. Evans, B. Halliwell, S.D. Brain, Formation and loss of nitrated proteins in peroxynitrite-treated rat skin in vivo, Biochem. Biophys. Res. Commun. 262 (1999) 781–786.
[32] M. Montalto de Mecca, E.G. Diaz, J.A. Castro, Nifurtimox biotransformation to reactive metabolites or nitrite in liver subcellular fractions and model systems, Toxicol. Lett. 136 (2002) 1–8.

Photochemistry and Photobiology, 2003, 77(4): 000–000

Base Oxidation at 5′ Site of GG Sequence in Double-stranded DNA Induced by UVA in the Presence of Xanthone Analogues: Relationship Between the DNA-damaging Abilities of Photosensitizers and Their HOMO Energies¶

Kazutaka Hirakawa[1], Mami Yoshida[1], Shinji Oikawa[2] and Shosuke Kawanishi*[2]

[1]Radioisotope Center, Mie University School of Medicine, Tsu, Mie, Japan and
[2]Department of Environmental and Molecular Medicine, Mie University School of Medicine, Tsu, Mie, Japan

Received 27 August 2002; accepted 12 January 2003

ABSTRACT

UVA contributes to skin cancer by solar UV light. Photosensitizers are believed to play an important role in UVA carcinogenesis. We investigated the mechanism of DNA damage induced by photoexcited xanthone (XAN) analogues (XAN, thioxanthone [TXAN] and acridone [ACR]), exogenous photosensitizers, and the relationship between the DNA-damaging abilities and their highest occupied molecular orbital (HOMO) energies. DNA damage by these photosensitizers was examined using ^{32}P-labeled DNA fragments obtained from the *p53* tumor suppressor gene. Photoexcited XAN caused DNA cleavage specifically at 5′-G of the GG sequence in the double-stranded DNA only when the DNA fragments were treated with piperidine, suggesting that DNA cleavage is due to base modification with little or no strand breakage. With denatured single-stranded DNA, the extent of XAN-sensitized photodamage was decreased. An oxidative product of G, 8-*oxo*-7,8-dihydro-2′-deoxyguanosine (8-*oxo*-dGuo), was formed by photoexcited XAN, and the 8-*oxo*-dGuo formation was decreased in single-stranded DNA. TXAN and ACR induced DNA photodamage as did XAN, although the order of DNA-damaging ability was XAN > TXAN > ACR. These findings suggest that photoexcited XAN analogues induce nucleobase oxidation at 5′-G of GG sequence in double-stranded DNA through electron transfer. The HOMO energies of these photosensitizers, estimated from *ab initio* molecular orbital (MO) calculation, decreased in the following order: XAN > TXAN > ACR. Extents of DNA damage increased exponentially with the HOMO energies of XAN analogues. This study suggests that DNA-damaging abilities of photosensitizers can be estimated from their HOMO energies.

INTRODUCTION

Solar UV light is a well-known carcinogen (1). UVB is directly absorbed by the DNA molecule to form cyclobutane pyrimidine dimmers and pyrimidine (6-4)-pyrimidone photoadducts (2,3). Recent studies have demonstrated that UVA also induces skin tumors in animals as does UVB (4). In addition, it has been reported that the mutagenic specificity of mutational spectrum of solar light in cells is not determined entirely by the UVB and that UVA greatly contributes to solar light–induced mutation (5). Because only little UVA can be absorbed by the DNA molecule, solar carcinogenesis would involve UVA-induced DNA damage mediated by endogenous or exogenous photosensitizers (or both) (6–9). We have previously demonstrated that in the presence of various photosensitizers, UVA causes DNA damage specifically at consecutive guanine through electron transfer (the Type I mechanism) (10–16).

Recently, *ab initio* molecular orbital (MO) calculation revealed the electron-donating site in B-form DNA to explain the sequence specificity of DNA photodamage (17,18). On the other hand, the approach of evaluating the DNA-damaging ability of photosensitizers using their energy of the highest occupied molecular orbital (HOMO) has not been well established. Various drugs or photosensitizers isolated from foods (or both) are believed to participate in solar carcinogenesis (19,20). Therefore, theoretical estimation of the risk of drugs or photosensitizer in foods (or both) as photocarcinogen should be important for cancer prevention. Calculated HOMO energy of photosensitizers is probably useful for estimating their DNA-damaging abilities through the Type I mechanism.

In this study, we investigated the mechanism of DNA photodamage induced by xanthone (XAN) analogues, exogenous photosensitizers and the relationship between the DNA-damaging abilities and their HOMO energies. Derivatives of XAN and its analogues, thioxanthone (TXAN) and acridone (ACR), have been isolated from various plants (21–25) and used as antitumor drugs (26). The mechanism of DNA damage induced by UVA irradiation in the presence of XAN analogues was examined using ^{32}P-labeled DNA fragments obtained from the *p53* tumor suppressor gene. We also measured the content of 8-*oxo*-7,8-dihydro-2′-deoxyguanosine (8-*oxo*-dGuo) (27), an oxidative product of 2′-deoxyguanosine (dGuo), formed by photoexcited XAN analogues with an

---

¶Posted on the website on

*To whom correspondence should be addressed at: Department of Environmental and Molecular Medicine, Mie University School of Medicine, Edobashi 2-174, Tsu, Mie 514-8507, Japan. Fax: +81-59-231-5011; e-mail: kawanisi@doc.medic.mie-u.ac.jp

Abbreviations: ACR, acridone; dGuo, 2′-deoxyguanosine; D_2O, deuterium oxide; DTPA, diethylenetriamine-*N*,*N*,*N*′,*N*″,*N*″-pentaacetic acid; HOMO, highest occupied molecular orbital; HPLC, high performance liquid chromatography; HPLC-ECD, electrochemical detector coupled to HPLC; MO, molecular orbital; $^1O_2$, singlet oxygen; $^{\cdot}OH$, hydroxyl radical; 8-*oxo*-dGuo, 8-*oxo*-7,8-dihydro-2′-deoxyguanosine; TXAN, thioxanthone; XAN, xanthone.

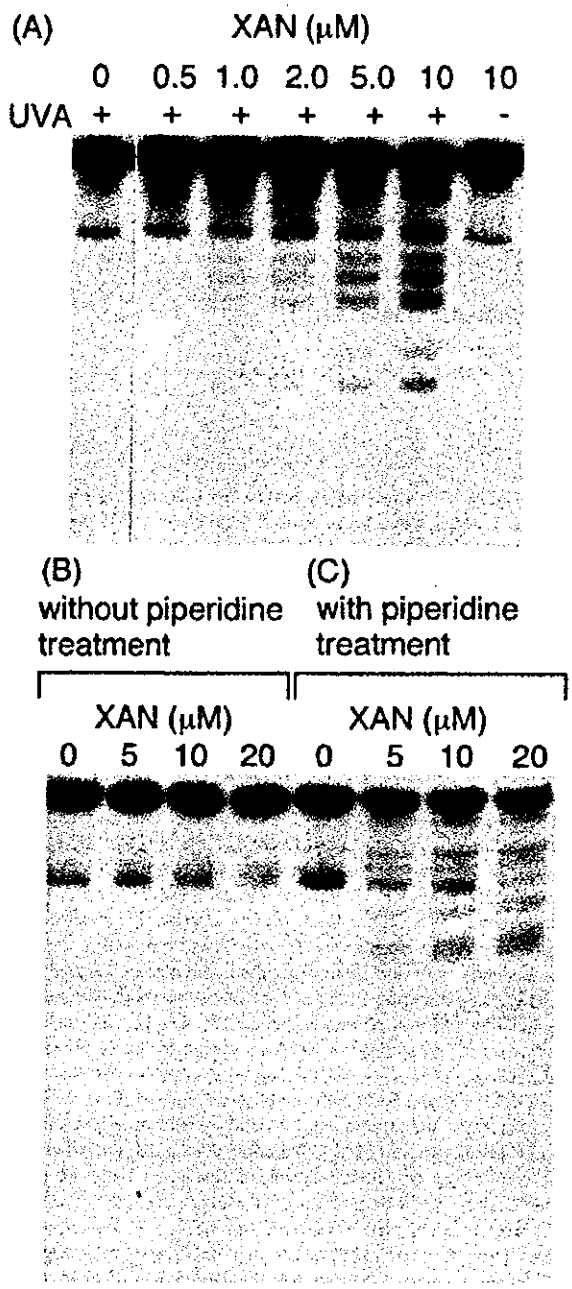

Figure 1. Autoradiogram of DNA fragments exposed to UVA light in the presence of XAN. The reaction mixture contained the ^{32}P-labeled 443 base pair (A) or 211 base pair (B,C) fragment, 20 μ*M*/base of calf thymus DNA, indicated concentration of XAN, 5 μ*M* DTPA and 2.5% (vol/vol) ethanol in 100 μL of 10 m*M* sodium phosphate buffer (pH 7.8). The reaction mixtures were exposed to 6 J·cm^{-2} UVA light (λ_{max} = 365 nm, 1.2 mW·cm^{-2}). Then, the DNA fragments were treated with (A,C) or without (B) 1 *M* piperidine and analyzed by the method described in Materials and Methods.

electrochemical detector coupled to high-performance liquid chromatography (HPLC-ECD). The HOMO energies of XAN analogues were estimated from *ab initio* MO calculation.

MATERIALS AND METHODS

Materials. Restriction enzymes (*Apa*I, *Hind*III and *Pst*I) and T4 polynucleotide kinase were purchased from New England Biolabs (Beverly, MA). Restriction enzyme (*Eco*RI) and calf intestine phosphatase were from Boehringer Mannheim GmbH (Mannheim, Germany). [γ-^{32}P]-ATP (222 TBq/mmol) was from New England Nuclear (Boston, MA). Diethylenetriamine-*N,N,N',N'',N''*-pentaacetic acid was from Dojin Chemicals Co. (Kumamoto, Japan). Calf thymus DNA was from Sigma Chemical Co. (St. Louis, MO). Nuclease P1 was from Yamasa Shoyu Co. (Chiba, Japan). XAN, ACR, acrylamide, bisacrylamide and piperidine were from Wako Chemicals Co. (Osaka, Japan). TXAN was from Acros Organics (New Jersey). Riboflavin was from Nacalai Tesque Co. (Kyoto, Japan). Deuterium oxide (D_2O) (99.95%) was obtained from Commissariat á l'Énergie Atomique in France.

Preparation of ^{32}P-5'-end-labeled DNA fragments. The DNA fragment of the *p53* tumor suppressor gene was prepared from pUC18 plasmid, ligated fragments containing exons of *p53* gene (28). The 5'-end-labeled 650 base pair (*Hind*III* 13972–*Eco*RI* 14621) fragment was obtained as described previously (29). This fragment was further digested with *Apa*I to obtain the singly labeled 443 base pair (*Apa*I 14179–*Eco*RI* 14621) and 211 base pair (*Hind*III* 13972–*Apa*I 14182) fragments. DNA fragments were also obtained from the human c-Ha-*ras*-1 proto-oncogene (30). The fragment was prepared from plasmid pbcNI, which carries a 6.6 kb *Bam*HI chromosomal DNA segment containing the c-Ha-*ras*-1 gene. The singly labeled 98 bp fragment (*Ava*I 2247–*Pst*I* 2344) was prepared as described previously (31). The asterisk indicates ^{32}P-labeling.

Detection of DNA damage induced by UVA in the presence of XAN analogues. The standard reaction mixture in a microtube (1.5 mL Eppendorf) contained XAN analogues, ^{32}P-labeled DNA fragment (0.2 ~ 1 μ*M*), 20 μ*M* calf thymus DNA, 5 μ*M* DTPA and 2.5% (vol/vol) ethanol in 100 μL of 10 m*M* sodium phosphate buffer (pH 7.8). Denatured single-stranded DNA fragments were prepared by heating at 90°C for 5 min followed by quick chilling before exposure to UVA light. The mixtures were exposed to 6 J·cm^{-2} UVA light under air using a 10 W UV lamp (λ_{max} = 365 nm, UVP, Inc., CA) placed at a distance of 20 cm. After the irradiation, the DNA fragments were treated with 1 *M* piperidine at 90°C for 20 min and treated as described previously (32). The DNA fragments were subjected to electrophoresis on an 8 *M* urea–8% polyacrylamide gel (20 V·cm^{-1}, 40 mA, 150–180 min). The autoradiogram was obtained by exposing an X-ray film to the gel. The preferred cleavage sites were determined by direct comparison of the positions of the oligonucleotides with those produced by the chemical reactions of the Maxam–Gilbert procedure (33) using a DNA sequencing system (LKB2010 Macrophor). A laser densitometer (LKB 2222 UltroScan XL) was used for the measurement of the relative amounts of oligonucleotides from treated DNA fragments. The relative yield of DNA photodamage was estimated from the absorbance of the bands in the fragmentation patterns of X-ray film.

Measurement of 8-oxo-dGuo formation induced by UVA in the presence of XAN analogues. The amount of 8-*oxo*-dGuo was measured by the method as described previously (12,27). The reaction mixtures containing 100 μ*M*/base calf thymus DNA, XAN analogues, 5 μ*M* DTPA, and 2.5% (vol/vol) ethanol in 4 m*M* sodium phosphate buffer (pH 7.8) were exposed to 6 J·cm^{-2} UVA light (λ_{max} = 365 nm) under air. After ethanol precipitation, DNA was digested to the nucleosides with nuclease P1 and calf intestine phosphatase and analyzed with an HPLC-ECD.

Calculation of HOMO energies of XAN analogues. HOMO energies of XAN, TXAN and ACR were estimated from *ab initio* MO calculation at Hartree–Fock 6-31G* level. Structures of these molecules were optimized by calculation of equilibrium geometry at Hartree–Fock 6-31G* level. These calculations were performed using Spartan '02 for Windows (Wavefunction Inc., CA).

RESULTS

UVA-induced DNA damage in the presence of XAN

DNA damage was induced by UVA irradiation in the presence of 0.5 μ*M* of XAN, and the extent of DNA damage increased depending on the concentration of XAN (Fig. 1A). XAN did not

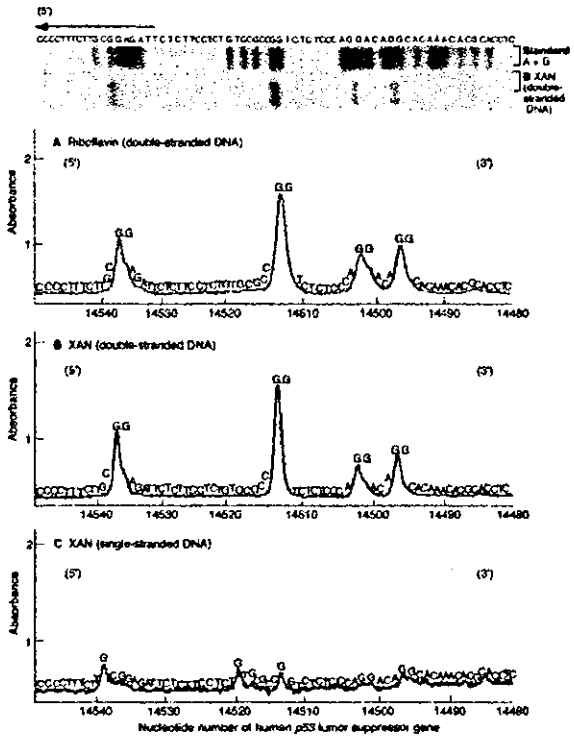

Figure 2. Sequence specificity of UVA-induced DNA damage in the presence of riboflavin or XAN. The reaction mixture contained the ^{32}P-labeled 443 base pair (*Apa*I 14179–*Eco*RI*14621) fragment, 20 μ*M*/base of calf thymus DNA, 5 μ*M* DTPA, 2.5% (vol/vol) ethanol, and 50 μ*M* riboflavin (A) or 10 μ*M* XAN (B,C) in 100 μL of 10 m*M* sodium phosphate buffer (pH 7.8). For the experiment with denatured single-stranded DNA, the ^{32}P-labeled and calf thymus DNA fragments were treated by heating at 90°C for 5 min followed by quick chilling on ice (C). The reaction mixtures were exposed to 6 J·cm^{-2} UVA light (λ_{max} = 365 nm, 1.2 mW·cm^{-2}). Subsequently, the DNA fragments were treated with 1 *M* piperidine. The DNA was analyzed and the relative amounts of oligonucleotides were measured by the methods described in Materials and Methods. Horizontal axis is the nucleotide numbers of the *p53* tumor suppressor gene.

induce DNA damage without UVA irradiation. DNA photodamage induced by XAN was observed only when the DNA fragments were treated with piperidine (Fig. 1B,C), suggesting that DNA damage is due to base modification with little or no strand breakage.

Typical hydroxyl radical (•OH) scavengers (ethanol, mannitol and sodium formate), catalase, and SOD showed no or little inhibitory effects on the DNA damage (data not shown). The DNA damage by photoexcited XAN was not enhanced in D_2O (data not shown). DNA damage induced by singlet oxygen ($^1O_2$) should be significantly enhanced by changing H_2O to D_2O (15,16) because the lifetime of $^1O_2$ is greatly enhanced in D_2O (from 4 μs in H_2O to 60 μs in D_2O) (34). Therefore, these results suggest that the contribution of reactive oxygen, such as •OH, hydrogen peroxide, superoxide anion radical and $^1O_2$ was negligibly small.

Sequence specificity of DNA damage by UVA in the presence of riboflavin or XAN

Figure 2 shows the sequence specificity of DNA damage induced by UVA in the presence of riboflavin, a Type I photosensitizer

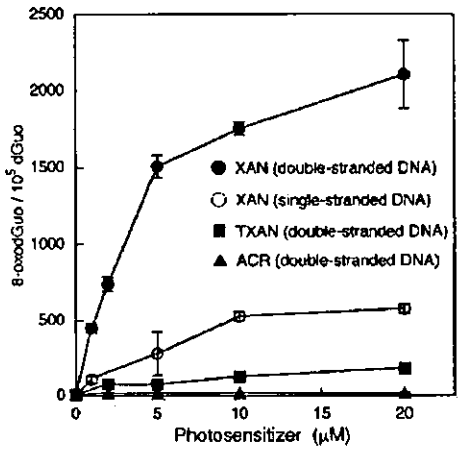

Figure 3. Formation of 8-*oxo*-dGuo induced by UVA in the presence of XAN analogues. The reaction mixture containing 100 μ*M*/base calf thymus DNA, indicated concentration of XAN analogues, 5 μ*M* DTPA and 2.5% (vol/vol) ethanol in 100 μL of 4 m*M* sodium phosphate buffer (pH 7.8) was exposed to 6 J·cm^{-2} UVA light (λ_{max} = 365 nm, 1.2 mW·cm^{-2}). Where indicated, the DNA fragment was denatured by heating for 5 min at 90°C followed by chilling on ice before UVA irradiation. After irradiation, the DNA was treated and the amount of 8-*oxo*-dGuo was measured by the methods described in Materials and Methods.

(12), or XAN. Photoexcited XAN as well as riboflavin caused DNA damage specifically at 5′-G of GG sequence in double-stranded DNA, suggesting that XAN induces DNA photodamage through the Type I mechanism. The band at 5′-AGGA between 14 510 ~ 14 500 nucleotide number was broadened, suggesting damage at both guanines. This is supported by the report that both guanines in a 5′-AGGA sequence were easily damaged through the Type I mechanism (35). With denatured single-stranded DNA, the extent of XAN-sensitized photodamage was decreased, and the damage occurred slightly at most guanine residues.

Formation of 8-*oxo*-dGuo by UVA in the presence of XAN analogues

Formation of 8-*oxo*-dGuo increased depending on concentration of XAN, and the amounts were clearly decreased by DNA denaturation (Fig. 3). The amounts of 8-*oxo*-dGuo formations in double-stranded DNA increased in the following order: XAN > TXAN > ACR.

Photon fluence dependence of DNA damage by photoexcited XAN

Formations of 8-*oxo*-dGuo, which is resistant to piperidine treatment, by photoexcited XAN increased depending on photon fluence controlled by the irradiation time (Fig. 4). The relative yield of piperidine-labile product appeared to be almost proportional to that of 8-*oxo*-dGuo within photon fluence of 3.7 × 10^{18} cm^{-2}. Larger amounts of photon irradiation increased the ratio of the yield of piperidine-labile product to that of 8-*oxo*-dGuo in a dose-dependent manner, suggesting further oxidation of 8-*oxo*-dGuo into piperidine-labile product.